



8th BALKAN CONGRESS OF NUCLEAR MEDICINE
ORAL PRESENTATIONS

[BSO-01]**A Prospective and Affordable Model with Comparable Accuracy to SPECT/CT in 90Y Dosimetry**

Mohammad Abuqbeith, Mustafa Demir, Özge Ulu, Özgür Taylan Akdağ, Burak Akovalı, Seçkin Bilgiç, Sait Sağer, Nami yeyin, Lebriz Uslu-Beşli, Kerim Sönmezoğlu

Istanbul University, Faculty of Cerrahpaşa Medicine, Department of Nuclear Medicine, Istanbul

Aim: Introduction of affordable and applicable model for 90Y dose planning as accurate as the advanced method using Tc-99m-MAA single photon emission computerized tomography (SPECT/CT). Also, the key-impact of scatter radiation and lung fraction (LF) from SPECT/CT were analysed with respect to the traditional LF from whole body scan.

Method: 15 patients (F=4, M=11) (6: colon Ca, 2: HCC, others: 7) were administered with 3-6 mCi Tc-99m-MAA for 90Y dosimetry. Afterward, Imaging protocol for whole body scan (WBS) was adjusted to include peakwindow and lower window with 15% width, followed by lung and Liver SPECT/CT. Lung fraction was calculated from scatter corrected (SC) SPECT/CT, SC-WBS, pixelwise SC SPECT, traditional WBS. DEW was adopted for scatter correction and designing a new model given as (SC-WBS) using special mathematical equation. The dose of healthy target and tumour was calculated using MIRD scheme over four vehicles: the standard SPECT/CT+LF (WBS), fully SPECT/CT, fully pixelwise SC SPECT, SPECT+ LF (SC-WBS).

Results: It was found that the lung fractions from both SPECT/CT and SC-WBS were less than the traditional LF from WBS by factor of 0.51 ± 0.11 and 0.47 ± 0.21 , respectively. An interesting correlation was detected in the lung fractions between SC-WBS and both SC SPECT/CT and SC SPECT ($R_1 = 0.93$ and $R_2 = 0.90$). The calculated absorbed dose (Gy/GBq) for the healthy target by SPECT/CT+LF (WBS), fully SPECT/CT based, fully pixelwise SC SPECT, SPECT with LF (SC-WBS), was 29 ± 17 , 31 ± 18 , 30 ± 18 , 32 ± 20 , and that for the tumour was 144 ± 41 , 155 ± 42 , 153 ± 44 , 146 ± 46 , respectively. Mann-Whitney test showed insignificant difference ($P_v \geq 0.05$) between the lung fractions from SPECT/CT and those derived from SC-WBS and pixelwise SC SPECT. While a significant difference was observed between all the methods and the traditional lungs fractions from WBS. Overall, there was no statistical difference between the methods in terms of the healthy target and the tumour dose.

Conclusion: Our study revealed a relevant variation $\approx 50\%$ (35-68%) in the computed lung fractions between the traditional WBS and those created by scatter corrected SPECT/CT. It has been emphasized that the introduced model involving SPECT for target and tumour quantification combined with scatter corrected WBS is an affordable, and applicable model to be recommended especially for 90Y therapy centers lacking integrated SPECT/CT.

Keywords: 90Y dosimetry, lung fraction, SPECT/CT, scatter correction

[BSO-02]**Relationship between Integrin $\alpha\beta 3$ and GRPR Tissue Levels and F-18 FDG PET/CT Findings in Patients with Breast Cancer**

Esra Arslan¹, Tamer Aksoy¹, Fadime Didem Can Trabulus², Canan Kelten Talu², Tevfik Fikret Çermik¹

¹University of Health Sciences, Istanbul Training and Research Hospital, Clinic of Nuclear Medicine, Istanbul

²University of Health Sciences, Istanbul Training and Research Hospital, Clinic of General Surgery, Istanbul

³University of Health Sciences, Istanbul Training and Research Hospital,

Department of Pathology, Istanbul

Aim: Gastrin releasing peptide (GRPR) and $\alpha\beta 3$ integrin receptors are known to be expressed in primary breast tumor tissue and metastatic tissue. There is a limited number of studies on the potential role of these receptors in molecular imaging. Aim of this study was to investigate the relationship between these receptors in cancerous tissues and their F-18 florodeoksilglukoz (FDG) positron emission tomography (PET/CT) parameters in histopathological and immunohistochemical subtypes of breast cancer.

Method: In this prospective study, the presence and level of GRPR and integrin $\alpha\beta 3$ receptors, in 90 tumor tissues of 87 breast cancer patients whose preoperative staging F-18 FDG PET/CT examinations performed between 2012-2018, were analyzed. Immunohistochemical scoring of GRPR and integrin $\alpha\beta 3$ receptors was performed as follows; none: 0, weak: 1, medium: 2 and strong: 3. According to the integrin $\alpha\beta 3$ receptor status, integrin $\alpha\beta 3$ score were divided to two groups as 0 (negative) and 1-2-3 (positive). In addition, the presence of ER, PR, Her-2 receptor obtained from breast tissue, GRPR and integrin $\alpha\beta 3$ receptor presence and level, ki 67%, histopathological subtypes were compared with the PET/CT findings like tumor size, axillary lymph node involvement, distal nodal metastasis, and presence of organ metastasis and F-18 FDG SUV_{max} of primary tumor.

Results: F-18 FDG involvement was observed in all of the 90 malignant breast lesions in PET/CT imaging. In the 75/90 breast tumor tissue, GRPR expression and 22/90 tissue integrin $\alpha\beta 3$ expression have been detected. In 6 tissues, both GRPR and integrin $\alpha\beta 3$ receptors were not detected. The relationships between primary tumors' SUV_{max} value and GRPR score 0,1,2 and 3 groups were presented Table1 and integrin $\alpha\beta 3$ score 0 and score 1-2-3 groups were presented in Table 2.

Conclusion: Although there was no statistically significant relationship between the GRPR score of 0,1,2,3 and the mean F-18 FDG SUV_{max} of the primary tumor, a negative trend was detected between the state of GRPR and the primary tumor F-18 FDG SUV_{max}. No statistically significant difference was found between the mean values of F-18 FDG SUV_{max} of integrin $\alpha\beta 3$ score 0 and score 1-2-3 tissues ($p > 0.05$). However, the high incidence and level of GRPR receptor positivity in breast cancer tissue suggests that this receptor may have potential role in molecular imaging and radionuclide therapy.

Keywords: Gastrin releasing peptide receptor (GRPR), $\alpha\beta 3$ integrin, F-18 FDG PET/CT, breast cancer

Table1. Relationship between GRPR scores and primary breast tumors F-18 FDG uptake

	Primary tumors SUV _{max} Mean \pm SD	p value
GRPR score 0 (n=15) GRPR score 1(n=27)	17.6 \pm 20.1 15.7 \pm 10.6	0.36
GRPR score 0 (n=15) GRPR score 2 (n=34)	17.6 \pm 20.1 13.9 \pm 8.4	0.19
GRPR score 0 (n=15) GRPR score 3 (n=14)	17.6 \pm 20.1 12 \pm 6.1	0.17
GRPR score 1 (n=27) GRPR score 2 (n=34)	15.7 \pm 10.6 13.9 \pm 8.4	0.23
GRPR score 1(n=27) GRPR score 3 (n=14)	15.7 \pm 10.6 12 \pm 6.1	0.12
GRPR score 2 (n=34) GRPR score 3 (n=14)	13.9 \pm 8.4 12 \pm 6.1	0.23
GRPR score 0 (n=15) GRPR score 1-2-3 (n=75)	17.6 \pm 20.1 14.5 \pm 11.0	0.14

Table 2. Relationship between Integrin $\alpha\beta 3$ scores and primary tumors F-18-FDG uptake

	Primary tumors SUV _{max} Mean \pm SD	p value
Integrin $\alpha\beta 3$ negative (n=68)	13.9 \pm 12.2	0.27
Integrin $\alpha\beta 3$ positive (n=22)	15.6 \pm 6.0	

[BSO-03]

PSMA Targeted Nuclear Robotic Surgery: Preliminary Results

Burçak Yılmaz¹, Selçuk Şahin², Nurhan Ergül¹, Halil Fırat Baytekin³, Yunus Çolakoğlu², Ali İhsan Taşçı², Tevfik Fikret Cermik³

¹University of Health Sciences, İstanbul Research and Training Hospital, Clinic of Nuclear Medicine, İstanbul

²University of Health Sciences, Bakırköy Dr. Sadi Konuk Research and Training Hospital, Clinic Of Urology, İstanbul

³University of Health Sciences, Bakırköy Dr. Sadi Konuk Research and Training Hospital, Clinic of Pathology, İstanbul

Aim: Prostate-specific membrane antigen (PSMA) targeted positron emission tomography/computed tomography (PET/CT) is successful imaging modality in prostate cancer (PC). But many centers do not have Germanium/Gallium (Ga)-68 generator and/or PET/CT. Also, reliable identification of small and/or atypically localized lymph nodes (Ln) during robotic surgery is challenging. In this prospective study, feasibility of tracer production using 99m-Tc-99m-PSMA-11 sterile cold kit, imaging procedure and accuracy with single photon emission tomography/computed tomography (SPECT/CT), technique and feasibility of Tc-99m-PSMA-11 radioguided robot-assisted laparoscopic radical prostatectomy (Tc-99m-PSMA-RG-RALRP) for Ln dissection of primary PC patients were evaluated.

Method: 5 primary PC patients with intermediate (n=2) or high (n=3) risk score who had PSMA receptor affinity according to Ga-68 PSMA-11 PET/CT were enrolled. Tc-99m-labelled PSMA-ligand (Tc-99m-PSMA-lEtS) was injected iv. (Mean 630 MBq; range 555-770 MBq activity). 61.6 \pm 7.8 min. after injection, SPECT/CT was performed. Mean time to start 99m-Tc-99m-PSMA-RG-RALRP with DaVinci XI robotic platform and laparoscopic gamma probe was 17 \pm 1.7 h. Radioactive rating of resected tissue was compared with postoperative histopathology. Physiological and pathological uptakes of organs and tissues for both imaging modalities were compared visually and quantitatively.

Results: Tc-99m-PSMA-lEtS was prepared in 2 hours with >96% purity and stability. 2 patients had suspicious Ln in PET/CT but not in SPECT/CT. Physiological radiotracer distribution were similar for both imaging modalities visually but PC lesions were much more visible on PET/CT. Mean operation time and mean console time were 6 h and 4.6 h, respectively. No patient suffered from complication related to surgery. After the 4th operation, in order to decrease urinary activity, Ln dissection was made prior to prostatectomy. Surgeons did not continue further superior Ln dissection when probe had no activity above than background. All dissected locoregional Lns were negative for metastasis; similar with per-operative probe results.

Conclusion: According to preliminary findings of this ongoing study, Tc-99m-PSMA-RG-RALRP seems to be of high value in patients with localized PC and loco-regional Ln which may shorten the operation time and make

surgeon feel more comfortable. Patient selection based on Ga-68 PSMA PET imaging is crucial.

Keywords: Gamma probe, prostate specific membrane antigen, radioguided surgery, PET/CT, SPECT/CT

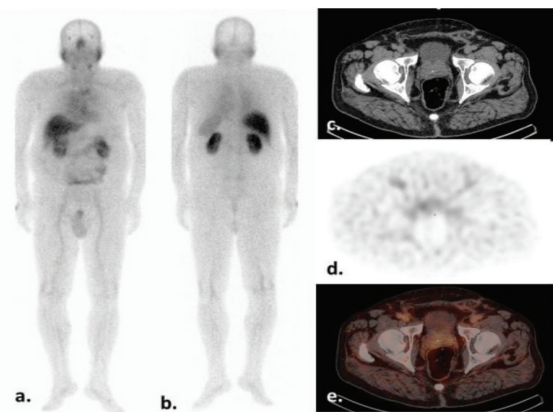


Figure 1. 99m-Tc PSMA-lEtS single photon emission computerized tomography imaging of 63 years old primary prostate cancer patient

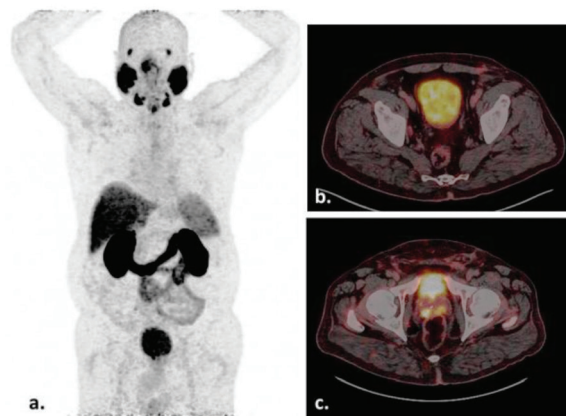


Figure 2. Ga-68 PSMA-11 positron emission tomography/computerized tomography imaging of 63 years old primary prostate cancer patient

[BGO-04]

The Role of Ga-68 DOTA-TATE and F-18 FDG PET/CT in the Follow-up Medullary Thyroid CA and Relationship with Tumor Markers

Onur Erdem Şahin, Rabia Lebriz Uslu-Beşli, Sertaç Asa, Emre Karayel, Hüseyin Pehlivanoğlu, Sait Sağer, Kerim Sönmezoglu

İstanbul University, İstanbul Faculty of Medicine, Department of Nuclear Medicine, İstanbul

Aim: Medullary thyroid cancer (MTC) is a more aggressive thyroid malignancy comparing to differentiated thyroid cancer. At the diagnosis local metastasis is present in 30-50% of the patients and 13-15% of the patients have distant metastasis, predominantly in the lung, liver and skeleton. In this study, we aimed to determine efficacy of F-18 florodeoksiglukoz (FDG)

positron emission tomography/computerized tomography (PET/CT) and Ga-68 DOTA-TATE PET/CT imaging in the patients with MTC and to evaluate relationship of imaging findings with calcitonin values.

Method: The records of MTC patients who were treated and followed-up in our department between 2005 and 2018 were retrospectively analyzed. Seventy-three patients with MTC who underwent either TATE PET/CT (n=176) or FDG PET/CT (n=125) scans associated with serum calcitonin and/or CEA measurement within 6 months period were included in the study. Additionally, TATE PET/CT (n=50) and FDG PET/CT (n=50) studies performed within 6 months on the same patient were re-analyzed separately for comparison of efficacy of both modalities (the comparison group).

Results: The overall sensitivity of FDG PET/CT images (n=125) was 67.8% in detecting recurrent or metastatic diseases, which is raised 77.6% in the subgroup of the patients with calcitonin levels >500 ng/L. On the other hand, TATE PET/CT scans (n=176) have an overall sensitivity of 81.4% in detecting for the detection of recurrent/metastatic diseases and this ratio is raised to 87.1% in patients with calcitonin levels >500 ng/L. In the comparison group, there was no significant difference in overall sensitivity (FDG PET/CT 64.6%, TATE PET/CT 70.8%, $p > 0.05$). However, TATE PET/CT was eligible to demonstrate significantly more bony lesions, comparing to FDG PET/CT scanning ($p = 0.014$).

Conclusion: Both FDG PET/CT and TATE PET/CT scans are efficient imaging modalities in detecting of recurrent/metastatic disease in MTC patients. However, TATE PET/CT scanning seems to be more sensitive for the detection of bone metastases in comparing to FDG PET/CT.

Keywords: Medullary thyroid cancer, FDG, DOTA-TATE, PET/CT, calcitonin

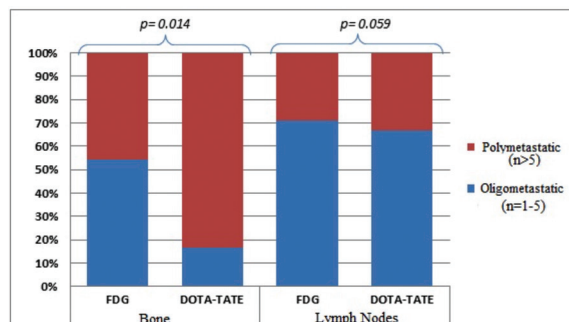


Figure 1. Lesion detection rates in comparison group

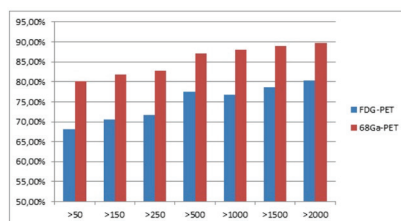


Figure 2. Sensitivities and relationship with calcitonin values

[BGO-05]

The Determination Presence of Immunohistochemical Prognostic Factors Via F-18 FDG PET Texture Analysis in Breast Cancer

Emine Acar¹, Bülent Turgut², Seyran Yiğit³, Gamze Çapa Kaya⁴

¹İzmir Kâtip Çelebi University, Atatürk Training and Research Hospital, Clinic of Nuclear Medicine; Dokuz Eylül University Institute of Oncology, Department of Translational Oncology, İzmir

²İzmir Kâtip Çelebi University, Atatürk Training and Research Hospital, Clinic of Nuclear Medicine, İzmir

³İzmir Kâtip Çelebi University, Atatürk Training and Research Hospital, Clinic of Pathology, İzmir

⁴Dokuz Eylül University Faculty of Medicine, Department of Nuclear Medicine, İzmir

Aim: The aim of this study was to determine the presence of immunohistochemical prognostic factors [estrogen receptor (ER), progesterone receptor (PR), her-2 status] non-invasively via texture analysis of the F-18 positron emission tomography/computerized tomography (PET/CT) images in locally advanced breast cancer.

Method: F-18 florodeoksiglukoz (FDG) PET/CT images of breast lesions 51 patients who were initially diagnosed with locally advanced breast invasive ductal adenocarcinoma were retrospectively analysed. Data from standardized uptake value (SUV)-based (5 data), volume-based (5 data), early texture analysis (9 data) and advanced texture analysis (41 data) were acquired using the PET images. Hormone receptor conditions were determined according to tru-cut biopsy results. Then, machine learning was performed on the textural features data set and immunohistochemical prognostic parameters with the utility of Naive Bayes and 3 different decision tree methods. Considering the branching points in the decision tree methods, some results were eliminated, then the machine learning was repeated.

Results: The mean age of the patients was 55 ± 13 years. There was estrogen receptor positivity in 34 patients, while 30 had progesterone receptor positivity and 25 had Her-2 positivity. According to the SUV, volume and texture analysis of the PET images, by machine learning method, the sensitivity, specificity, accuracy, positive predictive value and negative predictive value of ER positivity were calculated as 63-79%, 40-70%, 61-75%, 71-91%, 11-68% respectively, while PR positivity was estimated to be 60-72%, 47-70%, 55-67%, 54-90%, 32-68% and measured as 51-64%, 38-60%, 49-63%, 59-81%, 13-58% for Her-2 positivity.

Conclusion: In this study, the immunohistochemical factors in breast cancer were able to be determined non-invasively by using PET texture findings and machine learning. The most accurately estimated parameter by machine learning was estrogen positivity. We are of the opinion that that this method (reproducible at every stage of the disease) is promising as a result of leading to determine the intratumoral immunohistochemical prognostic factors by non-invasive evaluation of tumour and metastasis sites. This can aid clinicians in their decisions about hormonal therapy.

Keywords: Breast cancer, FDG, textural analysis, PET/CT, radiomics, machine learning

Table 1. Diagnostic accuracy

	Naive Bayes	J-48	Random forest	Random tree	Naive Bayes (selected parametres)	J-48 (selected parametres)	Random forest (selected parameters)	Random tree (selected parameters)	
ER	Sensitivity	67%	67%	71%	79%	63%	74%	69%	73%
	Specificity	63%	45%	61%	59%	40%	63%	70%	56%
	Accuracy	67%	61%	69%	71%	61%	71%	75%	67%
	PPV	90%	71%	84%	79%	91%	81%	91%	75%
	NPV	26%	42%	42%	68%	11%	53%	37%	53%
PR	Sensitivity	63%	71%	60%	63%	62%	72%	66%	60%
	Specificity	70%	61%	47%	50%	57%	58%	58%	48%
	Accuracy	65%	67%	55%	57%	61%	65%	63%	53%
	PPV	90%	69%	66%	59%	79%	62%	72%	54%
	NPV	32%	64%	41%	55%	36%	68%	50%	55%
Her-2	Sensitivity	51%	56%	59%	62%	51%	64%	58%	61%
	Specificity	50%	53%	54%	59%	38%	56%	56%	60%
	Accuracy	53%	55%	57%	61%	49%	63%	57%	61%
	PPV	81%	67%	59%	67%	81%	67%	70%	60%
	NPV	26%	42%	54%	54%	13%	58%	42%	50%

ER: Estrogen receptor, PR: Progesterone receptor, PPV: Positive predictive value, NPV: Negative predictive value

[BGO-06]

Induction of Oxidative/Nitrosative Stress Following Tc-99m Pertechnetate Thyroid Scintigraphy in Human

Ebru Salmanoğlu¹, Ergül Belge Kurutaş²

¹Kahramanmaraş Sütçü İmam University Faculty of Medicine, Department of Nuclear Medicine, Kahramanmaraş

²Kahramanmaraş Sütçü İmam University Faculty of Medicine, Department of Medical Biochemistry, Kahramanmaraş

Aim: Oxidative/nitrosative stress may be triggered by a various sources and ionizing radiation may also initiate oxidative/nitrosative stress. This is the first study, we aimed to investigate the induction of oxidative and nitrosative stress due to ionizing radiation in patients undergoing Tc-99m pertechnetate thyroid scintigraphy.

Method: Totally 26 patients (16 female, 10 male) undergoing Tc-99m pertechnetate thyroid scintigraphy were included in this study. The patients were aged between 20 and 50 years (58.0±16.3 years). The blood samples were taken from patients 20 minutes after intravenous injection of Tc-99m pertechnetate in dose used clinically (5 mCi) before the patients were taken to the thyroid imaging. Control group was selected from 30 healthy subjects (15 female, 15 male). The control group was aged between 17 and 72 years (57.0±14.0 years). The blood samples were taken both patients and control group for measuring antioxidant enzymes (catalase and superoxide dismutase), malondialdehyde, nitric oxide and nitrotyrosine as oxidative/nitrosative stress biomarkers.

Results: In this study we found that activities of antioxidant enzymes increased in patients compared to control (p<0.05). Further, malondialdehyde levels as an indicator of oxidative stress were higher in patients than control group (p<0.05). The levels of nitric oxide and nitrotyrosine as nitrosative stress biomarkers also increased in patients compared to control groups (p<0.05).

Conclusion: We thought that Tc-99m pertechnetate may cause an increase in reactive oxygen and nitrogen species and may cause oxidative/nitrosative damage at the cellular level. Our results indicated that the dose of Tc-99m pertechnetate given in these patients undergoing thyroid scintigraphy can tolerable.

Keywords: Radiation, nuclear medicine, oxidative/nitrosative stress, thyroid scintigraphy

8th BNMC ORAL PRESENTATIONS 1

[BOP-11]

Integration of Ga-68 PSMA PET/CT in Primary Therapy Decision Process in Localized Prostate Cancer

Hakan Akdere², Gül Ege Aktaş¹, Gürkan Arıkan², Ebru Taştekin³

¹Trakya University Faculty of Medicine, Department of Nuclear Medicine, Edirne

²Trakya University Faculty of Medicine, Department of Urology, Edirne

³Trakya University Faculty of Medicine, Department of Pathology, Edirne

Aim: The major change to evaluation in prostate cancer in AJCC is elimination of pT₂ substaging, defining a risk stratification in combination with tumor grade, prostate specific antigen (PSA). Also emerging data strongly suggest that a true volume measurement is more prognostically important than T₂ substaging. We evaluated the concordance of prostate specific membrane antigen (PSMA) positron emission tomography/computerized tomography (PET/CT) derived tumor volumes, target volumes, lymph node staging with histopathological results and the influence of integration of Ga-68-PSMA PET imaging into therapy decision.

Method: Twenty patients who had initial staging with Ga-68-PSMA PET and who had undergone radical prostatectomy, pelvic lymph node resection

between July 2016-September 2018 were retrospectively evaluated. We compared the gross tumor volume (P-GTV) derived from PSMA/PET with histopathologic (HP)-GTV and target volume with the knowledge of PSMA/PET with clinical target volume. Also, correlations between the parameters derived from PSMA PET/CT and prognostic factors effecting therapy decisions were evaluated. Finally we analyzed whether baseline PSMA/PET imaging led to a change of the TNM stage and final treatment plan.

Results: The mean HP-GTV and P-GTV were $14 \pm 14.03 \text{ cm}^3$ vs $13.66 \pm 11.80 \text{ cm}^3$ respectively. There was a strong correlation between the P-GTV's and HP-GTV's of the patients (intraclass correlation coefficient: 0.969, $p < 0.001$). Standardized uptake value (SUV_{max}) of the primary tumors were correlated with PSA values, HP-GTV's, TNM stages. Also GTV's were correlated with PSA values, SUV_{max} , tumor percentages. In 25% of the patients a change occurred in the pathologically confirmed TNM stage based on Ga-68 PSMA/PET. Finally 11 patients received adjuvant therapy due to the pT stage, surgical margin, lymph node positivity: in 5 (45%) of them the knowledge of PSMA PET/CT had changed the target volume. Additional radiotherapy was performed to the lymph nodes in these patients. Among these, 1 patient with non-regional lymph node, bone metastasis additionally had chemotherapy.

Conclusions: Integration of PSMA/PET into primary staging, therapy planning can be useful for selection of patients with high-risk-localized disease, who are seeking primary or salvage therapies. An initial PSMA/PET frequently leads to changes in the risk stage, altering the target volume or additional chemotherapy decision. Further studies are needed to analyze the impact of Ga-68-PSMA/PET based treatment planning on outcome and also for diagnostic (guided TRUS biopsy) purposes.

Keywords: PSMA/PET, prostate cancer, gross tumor volume, staging, treatment planning

Table 1. Dependence of upstaging on PSMA/PET on Tumor Grade, PSA levels and Roach formula

	Suspect of T ₃	Upstaged N-stage	Upstaged M-stage
Grad 1	2	1	0
Grad 2	3	2	0
Grad 3	2	2	1
Grad 4-5	1	0	0
PSA <10	0	0	0
PSA ≥10, <20	5	2	0
PSA ≥20	3	3	1
Roach formula <10%	1	0	0
10-15%	2	2	0
>15%	5	3	1

PSA: Prostate specific antigen

Table 2. Correlation of PSMA/PET/CT derived parameters with prognostic risk factors

	Histopathologic-GTV	PSA	Grade	Risk stage	Tumor percentage
SUV_{max}	r: 0.517*, p: 0.033	r: 0.580**, p: 0.009	r: 0.294, p: 0.222	r: 0.522*, p: 0.022	r: 0.356, p: 0.135
PET-GTV	r: 0.980**, p: 0.000	r: 0.564*, p: 0.012	r: 0.143, p: 0.558	r: 0.485*, p: 0.035	r: 0.699**, p: 0.001

PSMA: Prostate specific membrane antigen, PET: Positron emission tomography CT: Computerized tomography, SUV_{max} : Standardized uptake value, GTV: Gross tumor volume PSA: Prostate specific antigen

[BOP-12]

Comparison of Ga-68-PSMA PET/CT and Bone Scintigraphy for the Diagnosis of Bone Metastasis of Prostate Cancer

Müge Nur Engin, Duygu Has Şimşek, Caner Civan, Serkan Kuyumcu, Yasemin Şanlı

İstanbul University Faculty of Medicine, Department of Nuclear Medicine, İstanbul

Aim: The objective of this study was to investigate the diagnostic performance of Tc-99m bone scintigraphy (BS) in comparison to Ga-68-prostate specific membrane antigen (PSMA) positron emission tomography/computerized tomography (PET/CT) for the detection of bone metastases in prostate cancer patients.

Method: We enrolled 133 patients who underwent both BS and Ga-68-PSMA PET/CT within six weeks in our institution between April 2015 and November 2018. Bone lesions were evaluated by two experienced nuclear medicine physicians retrospectively and identified as benign, metastatic, or equivocal. For equivocal lesions on BS, single photon emission computerized tomography-CT (SPECT) images were also evaluated, if present. For final diagnosis, all equivocal lesions on both imaging were correlated with additional and follow up imaging (magnetic resonance, Ga-68-PSMA PET/CT, BS), clinical follow-up data and serum prostate-specific antigen (PSA) values.

Results: BS was negative in 69 (51.9%) of 133 patients and at least one metastatic or equivocal bone lesion was detected in remaining 64 (48.1%) patients. While no bone metastasis was observed in 87 (65.4%) patients, metastatic or equivocal bone lesions with Ga-68-PSMA uptake were detected in 46 (34.6%) patients, according to Ga-68-PSMA PET/CT findings. Equivocal lesions defined in BS were concluded as benign in 25 (18.7%) patients with correlative imaging. Equivocal lesions with PSMA uptake were confirmed as medullary infarction in femur and inflammation of rib fracture in 2 (1.5%) patients. Ga-68-PSMA PET/CT was able to detect more bone metastasis than BS in 16 (12%) patients. Five negative patients (3.7%) based on BS were upstaged to oligometastatic (n=3) or multimetastatic (n=2) disease with Ga-68-PSMA PET/CT findings. According to patient-based analysis, sensitivity, specificity, accuracy, positive predictive value and negative predictive value were 100%, 97.7%, 98.4%, 95.6%, 100% for Ga-68-PSMA PET/CT and, 88.6%, 71.9%, 78.9%, 60.9%, 92.7% for BS, respectively.

Conclusion: Our data indicate better diagnostic performance of Ga-68-PSMA PET/CT compared to BS for detection of skeletal disease extent. Ga-68-PSMA PET/CT effects the therapy management with the demonstration of undetected bone metastasis in BS, especially in oligometastatic/nonmetastatic disease. Depending on superior accuracy rates of our results, we presume that Ga-68-PSMA PET/CT is sufficient alone in the assessment of skeletal metastasis.

Keywords: Bone scintigraphy, Ga-68-PSMA PET/CT, prostate cancer

[BOP-13]

Comparative Study of Ga-68 PSMA PET/CT and Multiparametric MRI of Pelvis in Prostate Cancer staging

Muhammad Faraz Khaskhali, Hina Iqbal, Abdul Hai, Syed Rashid ul Amin, Adeen-ul-Hassan Rizvi

Sindh Institute of Urology And Transplantation

Aim: Early diagnosis of prostate cancer plays crucial role in proper planning and treatment. Structural imaging techniques like computerized tomography (CT) and magnetic resonance imaging (MRI) have established role in cancer staging but Ga-68-prostate specific membrane antigen (PSMA)-positron emission tomography (PET)/CT is superior for prostate cancer staging. Ga-68-PSMA PET/CT has high diagnostic accuracy for local and distant metastasis.

Our objective is to compare the Ga-68-PSMA PET/CT with MRI pelvis in prostate cancer staging and to evaluate the diagnostic Sensitivity, specificity, positive predicative value (PPV), negative predicative value (NPV), and accuracy of Ga-68-PSMA PET/CT using MRI as a gold standard.

Method: Total number of 40 patients of histologically proved prostatic adenocarcinoma who underwent MRI and Ga-68-PSMA PET/CT within 30 days was included in study.

Information from MRI and Ga-68-PSMA PET/CT of all patients were compared. Analysis was done on IBM SPSS vs22.

Results: Out of 40 patients, Ga-68-PSMA detects metastatic lymph nodes in 25 (62.5%) patients and MRI detects metastatic lymph nodes in 22 (55%) patients. PSMA detects the involvement of seminal vesicles in 30 (75%) patients and MRI detects in 23 (57.5%) patients. PSMA diagnostic sensitivity, specificity, PPV, NPV and accuracy for the detection of lymph nodes are 90.91%, 72.22%, 80.0%, 86.67% and 82.50% and for the detection of involvement of seminal vesicles are 95.83%, 56.25%, 76.67%, 90.0%, 80%.

Conclusion: From our results we concluded that Ga-68-PSMA PET/CT alone is better than MRI in determining the accurate staging of prostate cancer having good sensitivity and specificity. Ga-68-PSMA PET/CT is comparatively more superior imaging modality than MRI for the detection of local lesions. Furthermore Ga-68-PSMA PET/CT is also found to be more sensitive to find out metastatic lesion of prostate in different organs and other distant sites. So we expect that in the near future this study will be gold standard for prostate cancer staging.

Keywords: Ga-68-PSMA PET/CT, MRI, prostate cancer, comparison

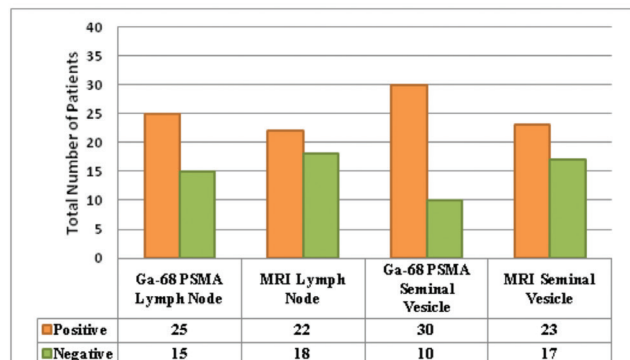


Figure 1. Detection of positive and negative metastatic lesions on Ga-68-PSMA and MRI

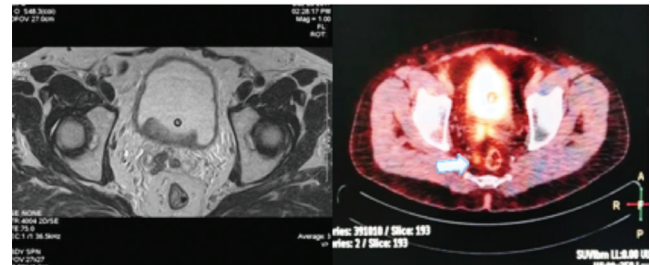


Figure 2. The comparison of PSMA image and MRI image

Diagnostic accuracy, sensitivity, specificity, PPV and NPV of Ga-68-PSMA PET/CT

S. No	Test	Lymphnode Detection on Ga-68 PSMA	Involvement of Seminal Vesicle on Ga-68 PSMA
1	Sensitivity	90.91%	95.83%
2	Specificity	72.22%	56.25%
3	Positive Predictive value	80.0%	76.67%
4	Negative Predictive Value	86.67%	90.0%
5	Accuracy	82.50%	80.0%

Ga: Gallium, PSMA: Prostate specific membrane antigen

[BOP-14]

Correlation of Ga-68-PSMA PET/CT Findings with PSA Values and Gleason Grades for Patients with Recurrent Prostate Cancer

İpek Öztürk¹, Gülin Uçmak², Aykut Kürşat Fidan³, Semra Demirtaş Şenlik², Burcu Esen Akkaş², Bedriye Büşra Demirel³

¹Şanlıurfa Mehmet Akif İnan Training and Research Hospital, Department of Nuclear Medicine, Şanlıurfa

²Dr. Abdurrahman Yurtaslan Ankara Oncology Training and Research Hospital, Department Of Nuclear Medicine, Ankara

³Karabük University Research and Training Hospital, Clinic of Nuclear Medicine, Karabük

Aim: Recurrence of prostate carcinoma after radical prostatectomy or other curative therapies is a common clinical problem especially in intermediate and high risk disease. Detecting the location and the extend of disease as early as possible is important for treatment planning and the clinical outcome. Traditional methods like computerized tomography (CT), Magnetic resonance imaging (MRI) and bone scan can be used for restaging but are known to show low sensitivity and specificity especially at low prostate specific antigen (PSA) values. In our study, we aimed to investigate the correlation between serum PSA values and Gleason grades and detectability of local-lymphatic, bone and visceral metastases on Ga-68-PSMA PET/CT and also the cut-off PSA values for PSMA PET positivity in both operated and non-operated patient groups.

Method: A total of 43 patients with prostate adenocarcinoma who were directed to our clinic for Ga-68-PSMA PET/CT scan were included in our study. Twenty patients were diagnosed with biochemical recurrence after radical prostatectomy (Group 1) and 23 were non-operated patients

diagnosed with biochemical failure after other treatment modalities (Group 2).

Results: The mean age of the 43 patients was 68.5 ± 8 (range: 53-83). Gleason grades were 1 in 1 patient (2.3%), 2 in 5 patients (11.6%), 3 in 10 patients (23.3%), 4 in 7 patients (16.3%) and 5 in 20 patients (46.5%). In Group 1, 9 out of 20 patients were PET positive (45%) and in Group 2, 21 out of 23 patients were PET positive (91%). PSA values ranged between 0.25-34.6 ng/mL in Group 1 and 1.0-3475 ng/mL in Group 2. Statistically significant correlation were detected between serum PSA values and PET positivity in both groups ($p < 0.001$). Optimal cut-off PSA value for PET positivity was 0.7 ng/mL in Group 1 and 2.1 ng/mL in Group 2. In addition, statistically significant correlation was observed between serum PSA levels and detection of lymph and bone metastases in Group 1. In Group 2, there was significant correlation between serum PSA levels and detection of lymphatic and visceral metastases. No correlation was detected between PET positivity and gleason grades.

Conclusion: In patients with biochemical recurrence, optimal cut-off values for Ga-68-PSMA PET/CT positivity were found for operated and non-operated patient groups separately. In both groups, disease was detected with high diagnostic accuracy even at low PSA values and we concluded that Ga-68-PSMA PET/CT has a very important role in patient management with recurrent prostate cancer.

Keywords: Ga-68-PSMA PET/CT, recurrent prostate cancer, PSMA

[BOP-15]

Ga-68-PSMA PET/CT in Reevaluation of Prostatic Ca within Low to High Level PSA Biochemical Recurrence

Evrin Abamor¹, Aysun Küçüköz Uzun¹, Tamer Atasever²

¹Istanbul Kartal Dr. Lütfi Kırdar Education And Research Hospital, Department of Nuclear Medicine, İstanbul

²Medipol Mega University Hospital, Clinic of Nuclear Medicine,

Aim: Evaluation of lesion detectability and efficacy of Ga68-PSMA PET/CT in restaging of Prostatic Ca within low to high prostate specific antigen (PSA) values of biochemical recurrence.

Method: We evaluated Ga-68-PSMA PET/CT findings of 135 patients (pt) (aged 53-87 yr; mean 70,16 yr) with biochemical recurrence of Pca, retrospectively. Gleason scores were between 6 to 10 (4 pt GS6 (3%), 57 pt GS7 (42%), 28 pt GS8 (21%), 39 pt GS9 (29%), 7 pt GS10 (5%). Patients were evaluated in seven groups according to PSA values (ng/mL): P1 (0,1-1), P2 (1-2) P3 (2-5), P4 (5-10), P5 (10-20), P6 (20-50) and P7 (PSA >50). Lesions were evaluated in four sites: primary region relaps, lymph node metastases in distant or regional, bone and soft tissue metastases. The detection rates of primary recurrence and metastates in all PSA groups and correlation ratio between PSA levels and lesion detection within all groups were analyzed.

Results: Overall detection rates of lesions are shown in Figure 1, where overall metastases were positive in 113 pt (83.70%). Detection rates of primary recurrence and regional metastases for PSA groups are shown in Figure 2 and Table 1. Strong correlation is shown in Table 1, between PSA increment and detection rates of primary recurrence, lymph node, bone and overall metastases. Very strong correlation was found between PSA increment and sof tissue metastasis rate (Table 1). Lymph node and primary recurrence rates were moderate in P3 and P4, while primary recurrence rate was significantly higher in groups with PSA >5ng/mL. Overall metastases rates were significantly higher in all PSA levels over 1 ng/mL. Soft tissue metastases were significantly higher in only P7 (PSA >50). Very strong correlation is found between primary recurrence rates and lymph node-

bone-overall metastases (Table 2). Where as there was moderate correlation for only soft tissue metastasis.

Conclusion: Ga-68-PSMA PET/CT is sensitive for detection of primary recurrence and lymph node metastasis in very low level (<1 ng/mL) biochemical recurrences, where early salvage therapy is important for improving prognosis. The detection rate for lymph node and bone metastases significantly rised in relatively low (1-2 ng/mL) biochemical recurrences in directing early systemic or local therapy. Ga-68-PSMA PET/CT should be recommended for reevaluation of disease with low level PSA relaps for early salvage and as well in higher levels of PSA relaps for restaging through systemic therapy planning.

Keywords: Ga-68-PSMA PET/CT, biochemical recurrence, prostatic carcinoma relaps

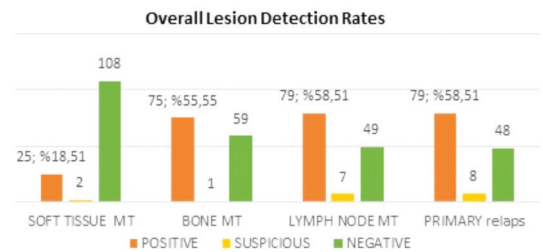


Figure 1.

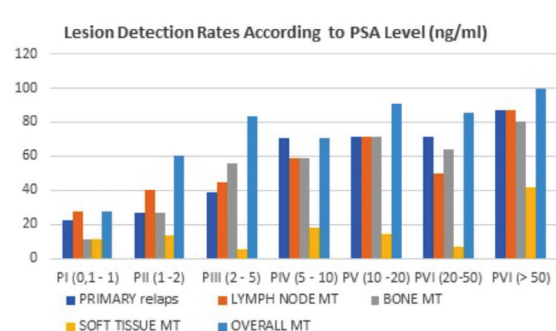


Figure 2.

Table 1. Detection rates of primary recurrence and metastases with correlation to PSA level

PSA level groups (ng/mL)	Primary Recurrence %	Lymph node met %	Bone met %	Soft tissue met %	Overall met %
P1 (0,1-1; mean 0,47)	22.22	27.77	11.11	11.11	27.77
P2 (1-2; mean 1,41)	26.66	40	26.66	13.33	60
P3 (2-5; mean 3,51)	38.88	44.44	55.55	5.55	83.33
P4 (5-10; mean 7,05)	70.58	58.82	58.82	17.64	70.58

P5 (10-20; mean 15.07)	71.42	71.42	71.42	14.28	90.47
P6 (20-50; mean 34.99)	71.42	50	64.28	7.14	85.71
P7 (>50; mean >100)	87.09	87.09	80.64	41.93	100
Correlation (r) with PSA increment	0.71	0.77	0.65	0.85	0.61

PSA: Prostate specific antigen

Table 2. Correlation (r) between primary recurrence rate and metastases rate

	Lymph node met	Bone met	Soft Tissue met	Overall met
Primary recurrence	0.89	0.92	0.57	0.80

[BOP-16]

Correlation of Ga-68-PSMA PET/CT Findings with Gleason Grades and PSA Values for the Primary Staging of Prostate Cancer

İpek Öztürk¹, Gülin Uçmak², Semra Demirtaş Şenlik², Aykut Kürşat Fidan³, Burcu Esen Akkaş², Bedriye Büşra Demirel²

¹Şanlıurfa Mehmet Akif İnan Research and Training Hospital, Şanlıurfa

²Dr. Abdurrahman Yurtaslan Ankara Oncology Research and Training Hospital, Clinic of Nuclear Medicine, Ankara

³Karabük University Karabük Research and Training Hospital, Clinic of Nuclear Medicine Karabük

Aim: Prostate specific membrane antigen (PSMA) is a transmembrane protein located mainly in the prostate tissue. PSMA expression is present in almost all primary and metastatic lesions of the adenocarcinomas of the prostate gland. With Ga-68-PSMA positron emission tomography/computerized tomography (PET/CT) scan, prostate cancer lesions can be detected with high diagnostic accuracy. PSMA expression is known to increase in aggressive disease. In our study, the correlation of standardized uptake value (SUV_{max}) values of primary prostatic lesion with serum PSA levels and Gleason grade and importance of SUV_{max} value in predictability of extra prostatic disease were investigated in the patients whom Ga-68-PSMA PET/CT were done for primary staging.

Method: Thirty-seven patients newly diagnosed with prostate adenocarcinoma by fine needle aspiration biopsy and referred to our clinic for Ga-68-PSMA PET/CT imaging for disease staging are included in our study. Their mean age was 65.6 (ranged 44-84). Gleason grades were 1 in 3 patients, 2 in 10 patients, 3 in 4 patients, 4 in 8 patients and 5 in 12 patients. Serum PSA values, Gleason grades and SUV_{max} value of primary lesions were noted.

Results: When statistical analysis were done, we found out that there was a statistically significant correlation between SUV_{max} value of primary lesion and Gleason grade (p=0.005) and also between SUV_{max} value of primary lesion and serum PSA values (p<0.001). In all cases, uptake of the primary tumor was detectable from nearby normal prostate tissue. Gleason grade

groups were found to be statistically significantly correlated with detection of lymphatic metastasis (p=0.04), on the other hand it was found that there was no correlation between Gleason grade and detection of bone metastasis. Also there was no statistically significant correlation between serum PSA levels and detection of lymphatic and bone metastasis. In addition, a statistically significant correlation was found between SUV_{max} values of the primary prostatic tumor and detection of metastasis. With an optimal SUV_{max} cut off value of 8.97, extraprostatic involvement can be predicted with 81.25% sensitivity and 66.67% specificity.

Conclusion: Ga-68-PSMA PET/CT is a diagnostic imaging tool useful in detecting prostate cancer lesions. PSMA expression, which is indicated by SUV_{max} is highly related with serum PSA values and Gleason scores, so that high expression may show more aggressive disease in primary staging.

Keywords: Ga-68-PSMA PET/CT, primary prostate cancer, PSMA

[BOP-17]

Comparison of Bone Scintigraphy and Ga-68-PSMA PET/CT in the Detection of Bone Metastases of Prostate Carcinoma

Çiğdem Soydal¹, Demet Nak¹, Mine Araz¹, Pınar Akkuş¹, Yüksel Ürün², Elgin Özkan¹, Nuriye Özlem Küçük¹, Metin Kemal Kır¹

¹Ankara University Faculty of Medicine, Department of Nuclear Medicine, Ankara

²Ankara University Faculty of Medicine, Department of Medical Oncology, Ankara

Aim: In this study, we aimed to evaluate the diagnostic performance of Ga-68-Prostate specific membrane antigen (PSMA) positron emission tomography/computerized tomography (PET/CT) in the comparison of planar bone scintigraphy (BS) in the detection of bone metastases, to determine if there is an additional benefit of BS in the patients who already underwent Ga-68-PSMA PET/CT and to define the role of additional information from Ga-68-PSMA PET/CT in the treatment planning.

Method: Forty-two patients with a median interval of 19 days between PSMA PET/CT and BS included to the analysis. Since histologic gold standard was absent for most of the cases, we defined best valuable comparator that is based on the consensus review of all available current and follow-up clinical data and imaging studies. For statistical analysis, the equivocal lesions were counted as negative (optimistic reading) or positive (pessimistic reading) in all imaging modalities.

Results: While BS was positive for bone metastases in 31 (67%) patients, PSMA PET/CT was positive in 24 (52%) patients. In the patient-based analysis sensitivity, specificity, accuracy, positive predictive value (PPV) and negative predictive value (NPV) for BS for detection of bone metastases were calculated as 50%, 19-29%, 32-39%, 32-39% and 33-39% whether equivocal findings were classified as positive or negative. For PSMA PET/CT these values were found significantly higher as 100%, 95-100%, 98-100%, 96-100% and 100%, respectively. In region-based analysis sensitivity and specificity for BS for detection of bone metastases were calculated as 70-80% and 15-80% whether equivocal findings were classified as positive or negative. For PSMA PET/CT these values were found significantly higher as around 100% and 100%. Further analysis on the diagnostic performance of BS and PET/CT were analyzed based on clinical subgroups. PSMA PET/CT was superior than BS in three groups. BS had higher sensitivity in staging and mCRPC groups than BCR. However, its specificity was lower in same indications. BS seems to have the highest accuracy in mCRPC group. In the staging group, based on the additional information from Ga-68-PSMA PET/CT the treatment strategy remained similar in two patients while it was changed from systematic to local in the 11/25 patients. In BCR group, the treatment strategy was changed from systemic to local in all of them.

Conclusion: In this retrospective study, PSMA PET/CT was found superior than planar BS in the detection of bone metastases. Additional information from PSMA PET/CT changes the treatment strategy in patients with BCR.

Keywords: Prostate carcinoma, bone scintigraphy, Ga-68-PSMA PET/CT.

[BOP-18]

Detection of Bone Metastasis of Prostate Cancer: Comparison Between PET and DWI Images in the Ga-68-PSMA PET/MR

Sertaç Asa¹, Rabia Lebriz Uslu Beşli¹, Eren Özgür², Barış Bakır², Kerim Sönmezoğlu¹

¹Istanbul University İstanbul Faculty of Medicine, Department of Nuclear Medicine, İstanbul

²Istanbul University İstanbul Faculty of Medicine, Department of Radiology, İstanbul

Aim: We aimed to compare positron emission tomography (PET) and diffusion weighted images (DWI) in the detection of bone metastases in prostate cancer patients who underwent Ga-68-Prostate specific membrane antigen (PSMA) PET/magnetic resonance imaging (MRI) in this retrospective study.

Method: A retrospective interpretation of 23 Ga-68-PSMA PET/MRI (1h after injection) of prostate cancer patients was performed. MRI sequences involved T1-weighted, hort tau inversion recovery, and (DWI-b: 1000). Two readers separately (nuclear medicine and radiology physician) evaluated both datasets regarding the characterization of bone lesions (negative, suspicious, positive). Both patients based and lesion-based analysis were performed (maximum 10 lesion/patient). All bone lesions were also correlated with computerized tomography (CT) if present.

Results: On patient-based analysis, we observed at least one abnormal lesion in 11 of 23 patients using both PET and DWI images. Among 64 lesions, that were detected using both imaging, 3/64 were negative and 61/64 were positive with PET; whereas DWI was negative in 12/64, suspicious in 2/64 and positive in 50/64 lesions. Among 12 lesions, that were PET positive and DWI negative; 10 of them had an additional CT scan, which confirmed sclerotic metastasis in 7 lesions and traumatic bone fractures in the rest of them. Re-evaluation of the DWI images of the remaining 2 lesions that were initially scored as PET positive and DWI negative was noticed to be positive on DWI images. Only one lesion was DWI positive and PET-negative and an additional CT image confirmed the presence of degenerative discopathy. Two bone lesions that were negative with PET and suspicious in DWI were confirmed to be false positive on CT. PET sensitivity, specificity, accuracy, Positive predictive value (PPV) and Negative predictive value (NPV) were 100%, 50%, 95%, 95% and 100%, respectively. Diffusion-weighted image sensitivity, specificity, accuracy, PPV and NPV were 84%, 50%, 81%, 94% and 25%, respectively.

Conclusion: PSMA PET has higher sensitivity, accuracy, and NPV in terms of bone metastasis detection compared to DWI.

Keywords: PSMA PET, PET/MRI, Prostate carcinoma

8th BNMC ORAL PRESENTATIONS 2

[BOP-21]

Clinical and Histopathological Evaluation of Incidental Focal Parotid Uptake Seen On FDG PET/CT

Zeynep Gül Kıpırak, Ayça Arçay, Gonca Gül Bural, Adil Boz, Metin Erkiş, Binnur Karayalçın

Akdeniz University Hospital, Clinic of Nuclear Medicine, Antalya

Aim: To evaluate the prevalence and clinical significance of focal parotid lesions with increased focal uptake identified on fluorodeoksiglukoz (FDG) positron emission tomography/ computerized tomography (PET/CT) in patients with non-parotid malignancies.

Method: FDG PET/CT images of 9.566 subjects performed between January 2016 to December 2018 were evaluated retrospectively. The ones with incidental focal FDG uptake in parotid gland with no prior history of primary parotid malignancies were noted. Clinical data was evaluated and the ones with pathology of parotid lesion were enrolled in the study. Maximum standardized uptake value (SUV_{max}) on PET images, patient demographics, clinical features, and histopathological diagnosis were evaluated for each subject.

Results: We detected 121 patients (18 female, 103 male) with incidental focal hypermetabolic parotid uptake on PET/CT. The prevalence of incidental focal hypermetabolic parotid uptake on PET/CT was 1.2% (121/9566). Twenty-two patients with incidental focal hypermetabolic parotid uptake had histopathological diagnosis. Malignancy was found in 1 (4.5%) of the patients, malignancy could not be excluded in 3 (13.6%) of the patients, benign pathology was detected in 18 (81.8%) of the patients (8 Warthin tumors, 2 oncocytomas, 8 other benign pathologies). The SUV_{max} mean ± standard deviation (SD) was 17.5±11 for benign lesions. The SUV_{max} of a single malignant lesion was 7.5. The SUV_{max} mean ± SD was 25.7±13.8 for the remaining 3 lesions pathologically suspicious for malignancy.

Conclusion: Focal increased FDG uptake on parotid is rarely noted on FDG PET/CT images. In our study, incidental focal hypermetabolic lesions in the parotid gland were more frequently seen in male. Even though the SUV_{max} values were high, many of these lesions were benign. There was no correlation between SUV_{max} value and malignancy in incidental parotid focal activity. Therefore focal increased FDG uptake on parotid may warrant further investigation to ensure accurate diagnosis.

Keywords: PET/CT, incidental focal hypermetabolic parotid uptake, parotid gland, parotid lesion pathology

[BOP-22]

The Value of Ga-68-PSMA PET-CT in Prostate Cancer as a Clinical Prognostic Factor

Duygu Has Şimşek, Yasemin Şanlı

Istanbul University, İstanbul Faculty of Medicine, Department of Nuclear Medicine, İstanbul

Aim: The aim of this study was to investigate the diagnostic power of Ga-68-Prostate specific membrane antigen (PSMA) positron emission tomography/computerized tomography PET/CT in the staging of prostate cancer (PC) and determine if a correlation exists between the PSMA uptake

of the primary tumor (PT) and prognostic factors.

Method: A total of 277 patients (mean age: 64 years; range: 44–93) with newly diagnosed PC [median prostate specific antigen (PSA): 16.4, GS: 6–10] who underwent Ga-68-PSMA PET/CT scan for staging were enrolled to this study. Patients were classified into risk groups according to the D'Amico risk stratification criteria. Images were reanalyzed by experienced nuclear medicine physicians. Lesions with PSMA uptake were categorized into benign, equivocal or metastatic. Correlative imaging, PSA values, follow up imaging and histopathological results were used for the final diagnosis of equivocal uptakes. PSA level and Gleason score (GS) were also compared with Ga-68-PSMA PET-CT findings using SPSS statistics version 24.

Results: According to D'Amico criteria, 6 patients (2.1%) were in low-risk group, 70 patients (25.2%) were in indeterminate risk group and 201 patients (72.7%) were in high-risk group. PT demonstrated positive PSMA uptake in 266 patients (96%). In 147 patients (53%), at least one positive metastatic lesion was detected outside the prostatic bed with Ga-68-PSMA PET/CT. Lymph node metastasis was detected in 112 patients (40.4%) and in 70 of patients (25.2%) were limited into the pelvis. Distant metastasis was seen in 81 patients (29.2%), that was mostly localized in bone. The SUV_{max} of PT was correlated with GS ($p < 0.001$) and D'Amico risk stratification ($p < 0.001$) according to the Kruskal-Wallis test. In addition, The SUV_{max} of PT was statistically higher in M1 disease versus M0 disease, according to the Mann-Whitney U test ($p = 0.016$). Finally, treatment strategies were changed in totally 128 patients (46.2%), with the demonstration of M1 disease in 81 patients (29.2%) and N1 disease in 47 patients (17%), based on Ga-68-PSMA PET/CT findings.

Conclusion: PC staging is significantly altered with PET/CT results, which affects therapy management in the present large cohort. Meanwhile, PSMA uptake of PT is correlated with GS, D'Amico risk stratification and metastatic status of disease, revealing that the SUV_{max} value of PT might be useful as a prognostic factor.

Keywords: Ga-68-PSMA PET/CT, prostate cancer, staging

[BOP-23]

PSMA PET/CT Staging in Patients with Intermediate Risk Prostate Cancer Those were Non-metastatic on Conventional Imaging?

Ömer Özsarac, Sevda Sağlampınar Karyağar

University of Health Sciences, Okmeydanı Training and Research Hospital, Clinic of Nuclear Medicine, İstanbul

Aim: The aim of this study was to evaluate the diagnostic contribution of the Ga-68-prostate specific membrane antigen (PSMA)-I&T positron emission tomography/computerized tomography (PET/CT) imaging in intermediate risk prostate cancer (PCa) patients those were non-metastatic on conventional imaging methods on pretreatment staging.

Method: A retrospective analysis was performed with 27 PCa patients (mean ages: 68.5; range: 54–78) those underwent a Ga-68-PSMA-I&T PET/CT scan for initial staging at our clinic from July 2017 to October 2018. Inclusion criteria of the patients were: a) intermediate risk PCa according to the D'Amico risk stratification system (Gleason score 7 [ISUP Grade 2/3] and serum prostate specific antigen (PSA) value < 20 ng/mL and cT_1 - T_2a/b tumor), b) non-metastatic on initial conventional imaging (such as multiparametric magnetic resonance imaging (MRI), abdominopelvic MRI/CT, bone scintigraphy), c) no prior therapies for PCa, d) no secondary malignancy.

Results: There were 14 patients with ISUP grade 2 PCa and 13 patients

with ISUP Grade 3. Serum PSA value were < 10 ng/mL in 16 patients and between 10–20 mg/mL in 11 patients. All of the 13 patients with ISUP grade 3 PCa had PSMA positive primary prostate lesion but 12 out of 14 patients with ISUP grade 2 PCa. Mean primary tumor SUV_{max} was 7.69 in ISUP grade 2 PCa (range: 2.4–17.48; median: 6.41) and 6.52 in ISUP grade 3 PCa (range: 3.2–18.49; median: 6.52). Mean primary tumor SUV_{max} was not different between patients with ISUP grade 2 and 3 ($p = 0.382$). Mean serum PSA value was 10.35 in ISUP grade 2 PCa (range: 3.59–18.06; median: 9.38) and 9.27 in ISUP grade 3 PCa (range: 4.25–17.49; median: 8.62). Mean serum PSA value was not different between patients with ISUP grade 2 and 3 ($p = 0.545$). On initial mpMRI, all of the primary tumors were positive but there were no pelvic enlarged lymph node compatible with metastasis in any patients on mpMRI or abdominopelvic MRI/CT. There was no patients who had increased pathological uptake that suggestive for metastasis on bone scintigraphy. On Ga-68-PSMA-I&T PET/CT imagings, only one patients (with ISUP grade 2 PCa, serum PSA value 10.16 ng/mL) had PSMA positive pelvic lymph nodes compatible with metastasis. But, PSMA positive metastatic bone lesion was not detected in any patient.

Conclusion: Metastases were rarely detected with Ga-68-PSMA-I&T PET/CT in intermediate risk PCa patients on whom any metastatic lymph node or metastases were not detected on pretreatment conventional imaging. Routine use Ga-68-PSMA-I&T PET/CT is not necessary for initial staging of this patients.

Keywords: PSMA PET/CT, intermediate risk PCa, metastasis, prostate cancer, D'Amico, Gleason score 7

[BOP-24]

Impact of Ga-68 PSMA PET/CT on Diagnosis of Hepatocellular Carcinoma

Cihan Gündoğan¹, Nurhan Ergül¹, Mehmet Semih Çakır², Tamer Aksoy¹, Nuri Özgür Kılıçkesmez², Tefvik Fikret Çermik¹

¹Istanbul Training and Research Hospital, Clinic of Nuclear Medicine, İstanbul

²Istanbul Training and Research Hospital, Clinic of Radiology, İstanbul

Aim: In this study, we investigated the diagnostic impact of staging Ga-68 prostate specific membrane antigen (PSMA) positron emission tomography/computerized tomography (PET/CT) on patients with hepatocellular carcinoma (HCC).

Method: Ten child pugh (CP)-A and 2 CP-B HCC patients [11 M, 1 F; mean age: 69 ± 5.9 (range: 58–76) years] were enrolled in this prospective study. All patients underwent PSMA PET/CT scan and F-18 fluorodeoxyglucose (FDG) PET/CT scan which performed within 30 days of each other. Magnetic resonance imaging (MRI) was performed to all patients before included in the study. The maximum standardized uptake value (SUV_{max}) was measured for primary tumors, lymph nodes and distant metastases in PSMA PET/CT and FDG PET/CT. In addition to SUV_{max} , tumor-to-liver (T/L) and tumor-to-background (T/B (gluteus medius muscle) taken into consideration. Liver tumors defined on PET/CT scans compared with MRI. Histopathology confirmed only in 4 patients.

Results: In PET/CT imaging, increased PSMA uptake was observed in 9 patients, mild uptake was observed in two patients and no uptake was observed in one patient [mean \pm standard deviation (SD) SUV_{max} 19.8 ± 12.4]. Four patients tumors were non-FDG avid, three patients showed mild FDG uptake and five patients showed increased FDG uptake (mean \pm SD, SUV_{max} 9.3 ± 5.6) (Table 1). PSMA uptake mean ratio for T/B was significantly higher in primary tumors compared with FDG ($p = 0.001$). However, PSMA uptake

mean ratio for T/L in primary tumors was higher than FDG, no significant difference was found ($p=0.26$). In our study group, 58 (98%) lesions were detected with PSMA PET/CT, while FDG PET/CT detected only 27 (46%) lesions. Seven (58%) patients had high-AFP-secreting tumors (>200 ng/mL) and 5 (42%) had low-AFP-secreting (<20 ng/mL) tumors. We did not find a relationship between AFP levels and PSMA or FDG uptake. Four patients had abdominal metastatic lymph nodes in PSMA PET/CT and one of them was non-FDG avid. Abdominal metastatic lymph nodes uptake in PSMA PET/CT was higher than FDG PET/CT in 3 of 4 patients. On the other hand, three patients had mediastinal lymph nodes metastases and these lesions FDG-PET/CT SUV_{max} levels are higher than PSMA PET/CT.

Conclusion: In patients with HCC, PSMA PET/CT is superior to FDG PET/CT as a molecular imaging modality, and we think PSMA PET/CT may be a potential new method in the diagnosis of primary tumors and metastatic lesions.

Keywords: Hepatocellular carcinoma, PSMA, FDG, PET/CT

Table 1.

Patient no	AFP Levels (μ g /L)	FDG uptake	PSMA uptake	FDG PET/CT Number of lesions	PSMA PET/CT Number of lesions
1	351	Mild	High	1	6
2	1643	Mild	High	2	2
3	4.7	High	High	1	1
4	7.8	Low	High	1	1
5	4.5	Low	High	1	1
6	1648	Low	Low	1	1
7	17.3	Mild	Mild	1	1
8	60473	High	Mild	1	2
9	205	High	High	4	>20
10	1042	High	High	12	>20
11	15195	High	High	1	2
12	10	Low	High	1	1

PSMA: Prostate specific membrane antigen, FDG: Fluorodeoxyglucose, PET: Positron emission tomography, CT: Computerized tomography

[BOP-25]

The Effectiveness of Positron Emission Tomography on Determining Gastrointestinal Pathologies

Didem Can Trabulus¹, Esra Arslan²

¹Istanbul Training and Research Hospital, Clinic of General Surgery, Istanbul

²Istanbul Training and Research Hospital, Clinic of Nuclear Medicine, Istanbul

Aim: Positron emission tomography/computerized tomography (PET/CT) is a highly effective imaging modality for cancer staging and follow-up. It allows detection of incidental pathologies as well as metastasis and local recurrences. In case of suspected gastrointestinal pathologies in PET/CT, the exact definition of the lesion is possible by endoscopy.

Method: Patients who were recommended gastrointestinal endoscopy in the PET/CT reports for the evaluation and follow-up of malignancy between December 2014 and November 2018 and who underwent upper and/or

lower gastrointestinal endoscopy were included in the study. The efficacy of PET/CT in detecting recurrent disease and incidental pathologies was investigated.

Results: Endoscopy was applied to 188 patients among 777 patients to whom gastrointestinal endoscopy was recommended in PET/CT reports. Of these patients, 34 had primary lung cancer, 11 had liver lung or bone metastasis with unknown primary, 37 had stomach, 24 had rectum, 20 had colon, 13 had breast, 9 had esophagus, 6 had liver hepatocellular carcinoma (HCC), 5 had larynx, 5 had pancreas, 4 had Hodgkin-non-Hodgkin's lymphoma, 2 had prostate, 2 had cervix, 2 had bladder, 2 had hypopharynx, 2 had intestine, 2 had sino-nasal, 1 had tonsil, 1 had thyroid, 1 had anal canal, 1 had ovary, 1 had duodenum, 1 had tongue, 1 had eyelid cancer. While 69 of the patients had normal gastrointestinal findings, 51 had signs of inflammation; polyps among 15 patients who had no primary gastrointestinal malignancy were detected. Local recurrences were seen among 4 patients with stomach and 3 patients with colon. New secondary gastrointestinal malignancy was detected among 8 patients without primary gastrointestinal tumor.

Conclusion: PET/CT is a very effective imaging modality for the detection of recurrent disease in the follow-up of gastrointestinal tumors and for the newly detection of incidental gastrointestinal pathologies. Definitive lesion recognition is provided with direct view with endoscopy.

Keywords: PET/CT, endoscopy, gastrointestinal tumors

[BOP-26]

Retrospective Investigation of Ga-68 Dotatate PET/CT on the Diagnosis of the Neuroendocrine Tumors and Treatment Approach

Selman Süreyya Sungur, Tamer Özüiker

University of Health Sciences, Okmeydanı Training and Research Hospital, Clinic of Nuclear Medicine, Istanbul

Aim: Ga-68 labeled DOTA peptides are more sensitive than single photon emission computerized tomography (CT) agents for neuroendocrine tumor (NET's) imaging. We aimed to evaluate the efficacy of Ga-68 DOTA-TATE positron emission tomography (PET)/CT imaging on NET and determine its contribution of treatment decisions.

Method: We evaluated 53 (52 histopathologically, 1 clinical) NET patient's Ga-68 DOTA-TATE PET/CT scans, treatment history before and after imaging and calcitonin levels [for medullary thyroid carcinoma (MTC)] retrospectively. Each uptake that is higher than background and outside of the physiological region was accepted as pathological and their standardized uptake value (SUV_{max}) values were measured. They were discriminated with clinical, histopathological and other imaging as malignant and benign. Sensitivity and PPD both patient and lesion-based were calculated. Therapy changes before and after the scan were determined. SUV_{max} of lesions were analyzed between G1, G2 and G3 groups. Additionally, correlation between ki-67 index of known lesions and their SUV_{max} values were analyzed. Therapy change, sensitivity and PPD were also calculated for MTC. Correlation between counts of malignant lesions and calcitonin levels were analyzed for bones, lymph nodes, visceral organs and whole.

Results: The lesion based sensitivity of Ga-68 DOTA-TATE PET/CT was 96.8% (PPD: 64.2% false negative: 2%). Mean SUV_{max} of tumors of G1 patients was significantly higher than tumors of G3 patients statistically ($p=0.033$). We found a negative correlation between SUV_{max} and ki-67 index of lesions that detected on PET/CT but it wasn't significant statistically ($p>0.05$). The lesion based sensitivity in MTC was 96.8% (PPD: 60%, false negative: 1.9%)

There was a positive correlation between calcitonin level and count of malignant lymph nodes and whole malignant lesions that were detected on PET/CT. Therapy changes were 57.7% for all patients. The most common decision were surgery, SSA initiation and PRRT respectively.

Conclusion: Ga-68 DOTA-TATE PET/CT has high sensitivity for evaluation NET and MTC lesion based. Lesions of G1 patients have higher SUV_{max} than G3 patients have (p=0.033). Ga-68 DOTA-TATE PET/CT has an important impact for treatment decision. There is a negative relation between the ki-67 index and SUV_{max} but it's not significant (p>0.05). There is a significant correlation between the calcitonin level and the number of metastatic lymph nodes and the total number of malignant lesions (p=0.007, p=0.006). High calcitonin levels can be a predictor for lymph node metastasis.

Keywords: Ga-68 DOTA-TATE, treatment management, neuroendocrine tumor, ki-67, efficacy

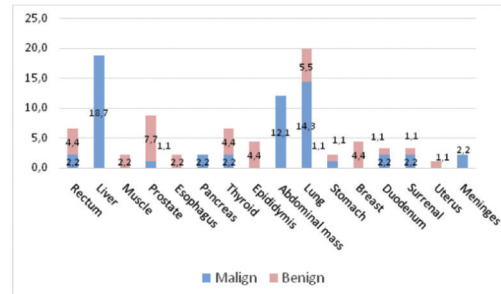


Figure 2. Distribution percentages of malignant and false (+) lesions of visceral organs on Ga-68 DOTA-TATE PET/CT

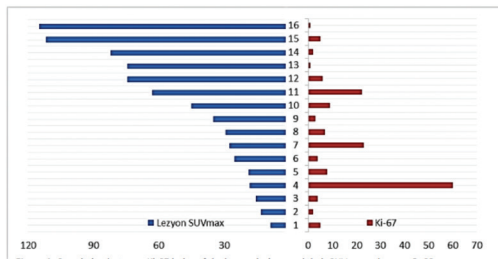


Figure 1. The relationship between lesion SUV_{max} and ki-67 index

Table 1. Clinical characteristics of the patients and therapy change and patient-based results of Ga-68 DOTA-TATE PET/CT

	n	Primary Site	n	Primary Site	n
Sex (n)	-	Unknown	8	Duodenum	2
Male	16	Lung	3	Pancreas	4
Female	37	Thyroid	21	Small bowel	1
Age (y)	-	Esophagus	1	Colon	2
Median	58	Stomach	6	Surrenal	2
Range	32-68	Over	1	Appendix	1
Ki-67 index (%)	-	-	-	-	-
Median	5	-	-	-	-
Range	1-95	-	-	-	-
			Ga-68 DOTA-TATE PET/CT		
	n	Therapy Change	True (+)	False (+)	Negative
All patients	53	57.7	40	11	2
GEP-NET (foregut)	13	50	7	4	2
GEP-NET (migdut)	1	0	1	-	-
GEP-NET (hindgut)	3	100	2	1	-
MTC	21	42.8	16	5	-
Lung NET	3	100	3	-	-
Other NET (surrenal, over)	3	66.6	2	1	-
Carcinoid syndrom related NET	1	100	1	-	-
Unknown primary	8	75	8	-	-
Grade (n=30)	-	-	-	-	-
G1	8	25	4	3	1
G2	13	83.3	10	2	1
G3	9	77.8	8	1	-

MTC: Medullary thyroid carcinoma, NET: Neuroendocrine tumor

Table 2. Lesion-based analysis of the patients according to Ga-68 DOTA-TATE PET/CT

Number of lesions of all patients for...	n	True (+)	False (+)	Sensitivity	PPD	False (-)
Overall (n)	342	215	120	96.8%	64.2%	2%
Bone	124	116	8	100%	93.5%	-
Lymph nodes	127	51	76	100%	40.1%	-
Visceral organs	91	48	36	87.3%	57.1%	7.7%
Comparison of SUV_{max} between grades of the patients						
Grade of patients	n	Mean SUV _{max}	Comparison	p value		
G1	9	40.23	1 vs. 2	0.121	-	-
G2	60	22.47	2 vs. 3	0.409	-	-
G3	50	13.53	1 vs. 3	0.033*	-	-
Correlation between number of malignant lesions and calcitonin levels in MTC						
		Calcitonin				
Bone	r=0.365	p=0.104	-	-	-	-
Lymph nodes	r=0.570	p=0.007*	-	-	-	-
Visceral organs	r=0.191	p=0.408	-	-	-	-
Total	r=0.576	p=0.006*	-	-	-	-

Ga: Gallium, PET: Positron emission tomography CT: Computerized tomography, SUV: Standardized uptake value, MTC: Medullary thyroid carcinoma

[BOP-27]**Evaluation of Hypermetabolic Thyroid FDG PET Nodules Using EU-TIRADS a New Approach**

Ayça Arçay, Zeynep Gül Kırprak, Gonca Gül Bural, Adil Boz, Metin Erkilic, Binnur Karayalçin

Akdeniz University Hospital, Clinic of Nuclear Medicine, Antalya

Aim: The aim of this study is to reevaluate the ultrasound (US) findings of incidental hypermetabolic thyroid nodules using EU-TIRADS criteria and correlate the outcome with histopathology.

Method: Three thousand seven hundred ninety-three florodeoksiglukoz (FDG) positron emission tomography/computerized tomography (PET/CT) images performed in our department between September 2017 and December 2018 were evaluated retrospectively. Three hundred and twenty-eight subjects with focal increased FDG uptake in thyroid lesions were noted. The ones who had fine needle aspiration biopsy (FNAB) results were enrolled in the study. US findings of these lesions were reevaluated using EU-TIRADS criteria. Standardized uptake value (SUV_{max}) of each focal thyroid lesion and SUV_{max} ratio (SUV_{max}/thyroid background activity) were calculated. These findings were correlated with FNAB results and their relationship were evaluated retrospectively.

Results: Fifty-six hypermetabolic thyroid nodules in 46 patients were examined. The FNAB results were: 7 malignant, 5 suspicious for malignancy, 31 benign and the remainings were non-diagnostic. The SUV_{max} and SUV_{max} ratio median values of 12 focal activities which were found as malignant and suspicious for malignancy were 14.08 and 7.94, respectively; SUV_{max} and SUV_{max} ratio median values of 31 focal activities which were found as benign were 7.1 and 4.33, respectively. SUV_{max} and SUV_{max} ratio values were greater in the malign group than the benign group (Mann-Whitney U test, p=0.002 and p=0.024, respectively). The cut-off value of SUV_{max} and SUV_{max} ratio discriminating benign and malignant lesions were calculated using ROC analysis and were detected as 10.35 (with 83% sensitivity and 78%

specificity, p=0.002) and 6.12 (with 66% sensitivity and 71% specificity, p=0.007), respectively. Malignancy ratios in different EU-TIRADS groups are given at Table 1. Sensitivity, specificity, positive predictive value, negative predictive value and accuracy ratios for malignancy of three groups SUV_{max} >10.35, SUV_{max} ratio >6.12 and EU-TIRADS 5 are given at Table 2.

Conclusion: EU-TIRADS criteria can discriminate the lesions at high risk for malignancy from those at low risk among hypermetabolic thyroid nodules incidentally detected on FDG PET/CT. Additionally, using a predetermined cut-off value for SUV_{max} and SUV_{max} ratio could further enhance our interpretation in the differentiation of benign and malignant thyroid nodules.

Keywords: Hypermetabolic thyroid nodules, incidental focal uptake in thyroid, FDG PET/CT, EU-TIRADS, FNAB

Table 1. Malignancy ratios in different EU-TIRADS groups

	Number of malign nodules	Malignancy ratio
EUTIRADS 5 (15 focal activities)	6/15	40%
EUTIRADS 4 (14 focal activities)	2/14	14%
EUTIRADS 3 (11 focal activities)	0/11	0%

Table 2. Sensitivity, specificity, PPV, NPV and accuracy ratios of three groups for malignancy

	Sensitivity	Specificity	PPV	NPV	Accuracy
SUV _{max} >10.35	83.3%	75%	47.6%	94.2%	76.7%
SUV _{max} ratio >6.12	66.6%	70.4%	38%	88.5%	69.6%
EUTIRADS 5	75%	71.8%	40%	92%	72.5%

8th BNMC ORAL PRESENTATIONS 3

[BOP-32]

[BOP-31]

F-18-Choline PET/CT Can Be a Useful Tool to Differentiate Malignant-Benign Thyroid NodulesMine Araz¹, Demet Nak¹, Çiğdem Soydal¹, Sevim Güllü², Özlem N. Küçük¹¹Ankara University Faculty of Medicine, Department of Nuclear Medicine, Ankara²Ankara University Faculty of Medicine, Department of Endocrinology and Metabolism Diseases, Ankara

Aim: There have been efforts to differentiate malignant thyroid nodules from benign nodules by molecular imaging, mainly Tc-99m methoxyisobutylisonitrile scintigraphy. Positron emission tomography/computed tomography (PET/CT) with F-18 or C-11 labelled choline has been used for imaging prostate carcinoma for some time and recently for detection of parathyroid adenoma in hyperparathyroidism. There are some case presentations where incidental focal thyroid uptake of F-18/C-11 choline have been reported as either benign thyroid nodules or primary thyroid malignancies. One recent study has also evaluated the clinical importance of incidental choline uptake in the thyroid. In this study, we investigated the distribution of F-18-choline uptake in thyroid nodules with either benign or malignant cytology.

Method: All F-18-choline (FCH) PET/CT studies performed for evaluation of hyperparathyroidism etiology in Ankara University Faculty of Medicine, Department of Nuclear Medicine between November 2017-December 2018 were retrospectively reevaluated. Patients with coexisting thyroid nodules and histopathological examination results are involved.

Results: Among 468 F-18-FCH PET/CT studies, 60 patients had coexisting nodular thyroid disease. Thyroid fine needle aspiration biopsy, lobectomy or thyroidectomy results could be obtained in 18 patients (male: 2, female: 16, mean age: 58.71±8.58). Thyroid papillary carcinoma was detected in 4/18 patients, FLUS in 1/18 patients and benign in 13/18 patients. Mean SUV_{max} of thyroid nodules with papillary carcinoma were 4.12 (minimum: 2.3-maximum: 7.2). Mean largest size of the tumor was 6.83 mm (minimum: 4 mm, maximum: 11 mm). The tumor with the highest diameter had the highest SUV_{max}. Patient with FLUS had a nodule of 8 mm and SUV_{max}: 4.2. Benign nodules had a mean SUV_{max}: 2.35 (minimum: 1.7, maximum: 5.1). Although mean SUV_{max} levels of benign nodules seem to be lower than malignant nodules, statistical analysis could not be performed due to small number of patients. The overlap between SUV_{max} of benign and malignant nodules may be due to relatively lower F-18-choline uptake in papillary tumors less than 10 mm, that is, the partial volume effect.

Conclusion: F-18-choline uptake seems to be higher in malignant nodules compared to benign nodules. Incidental F-18-choline uptake in thyroid should be further evaluated. F-18-choline may be helpful to differentiate benign-malignant nodules, especially when FNAB is reported as FLUS, if supported with further prospective data.

Keywords: PET/CT, thyroid nodule, neoplasms

F-18-FET and F-18-choline PET/CT in Patients with Newly Diagnosed Low-Grade Gliomas: A Pilot StudyMarina Hodolić¹, Ana Mišir Krpan², Anja-Tea Golubić³, Marijan Žuvić³, Maja Baučić², Goran Mrak⁴, Jakob Nemir⁴, Dražen Huić⁴¹Nuclear Medicine Department, Faculty of Medicine and Dentistry, Palacký University Olomouc, Czech Republic; Nuclear Medicine Research Department Iason, Graz, Austria²Department of Oncology, University Hospital Centre Zagreb, Croatia³Department of Nuclear Medicine And Radiation Protection, University Hospital Centre Zagreb, Croatia⁴Department of Neurosurgery, University Hospital Centre Zagreb, Croatia

Aim: Low grade gliomas (LGG) account for app. 15% of all gliomas. Most LGG gradually evolve into high grade tumours.

Method: fMRI results are often inconclusive, ambiguous or indeterminate. The definitive diagnosis can be achieved by brain biopsy, which is invasive, inaccessible, associated with sampling errors.

Results: O-[2-(F-18)-fluoromethyl]-L-tyrosine (F-18-FET) has been recently approved in EU as a positron emission tomography (PET) radiopharmaceutical for characterisation of brain lesions suggestive of gliomas. F-18-FET has advantage of displaying a high tumour-to-background ratio and not accumulating in inflammatory lesions. Because of low uptake in normal brain parenchyma, fluoromethyl-(F-18)-dimethyl-2-hydroxyethyl-ammonium chloride F-18-fluorocholine (FCH) has proven to be a good alternative in centres where F-18-FET is not available.

No study has been published on the use of F-18-FCH and F-18-FET in primary diagnosis of LGG. The objective of this pilot study was to determine accuracy of primary diagnosis of LGG with choosing the appropriate PET radiopharmaceutical.

This pilot study comprised 8 patients (age 37-80 years) with suspected LGG, diagnosed with 3T MRI and/or stereotactic-brain-biopsy. After fMRI and/or stereotactic-brain-biopsy all patients underwent F-18-FCH and F-18-FET PET/computerized tomography (CT) within one week. Patients underwent surgery within one to two weeks after PET/CT. Pathohistological results were compared with F-18-FCH and F-18-FET PET/CT findings. Seven out of eight patients had full imaging diagnostics with final pathohistological findings after surgery. Five of them were fMRI and pathohistologically diagnosed as LGG: four were positive on F-18-FET [standardized uptake value (SUV_{max}): 1.7; 2; 2.8 and 1.8] and negative on F-18-FCH PET/CT. One patient with pathohistologically proved LGG had negative F-18-FET and negative F-18-FCH PET/CT. Two patients diagnosed as LGG on MRI were confirmed as glioblastoma multiforme after surgery: both of them were positive on F-18-FCH (SUV_{max} 3.9 and 1.6) and F-18-FET (SUV_{max} 3.1 and 3) PET/CT. The last patient who entered this study had negative F-18-FCH and positive F-18-FET (SUV_{max} 1.5) PET/CT but has no final pathohistological diagnosis yet.

Conclusion: Preliminary results based on a small number of patients showed that appropriate radiopharmaceutical should be chosen before performing PET/CT in patients with newly diagnosed LGG. F-18-FCH seems not to be appropriate tracer in patients with newly diagnosed LGG. Both tracers, F-18-FCH and F-18-FET, seems to be appropriate in primary diagnosis of high grade gliomas. The study is ongoing.

Keywords: F-18-FET, 18F-choline, PET/CT, low-grade gliomas

[BO-P33]**Detecetability of F-18-Choline PET/MR in Primary Hyperparathyroidism with Negative Neck Ultrasound and Tc-MIBI SPECT**

Mine Araz¹, Demet Nak¹, Çiğdem Soydağ¹, Elif Peker², İlhan Erden², Sevim Güllü², Özlem N Küçük¹

¹Ankara University Faculty of Medicine, Department of Nuclear Medicine, Ankara

²Ankara University Faculty of Medicine, Department of Radiology, Ankara

³Ankara University Faculty of Medicine, Department of Endocrinology and Metabolism Diseases, Ankara

Aim: To evaluate the power of 18F-fluorocholine (FCH) positron emission tomography/magnetic resonance (PET/MR) imaging in primary hyperparathyroidism.

Method: Twenty consecutive patients (female: 12, male: 8, mean age: 48.65±14.93) with primary hyperparathyroidism who were referred to Ankara University Faculty of Medicine, Department of Nuclear Medicine for F-18-FCH PET/MR study were included in the study. All patients had previously undergone neck ultrasound (USG) and Tc-99m metoxyisobutylisonitrile (MIBI) scintigraphy but parathyroid adenoma could not be localised.

Results: Mean levels of serum PTH and Cancer were: 85±29.9 and 10.7 respectively. 18F-FCH PET/MR was positive for a parathyroid adenoma in 17/23 patients. In 6/17 patients, 18F-FCH PET/computerized tomography (CT) was also found negative. Parathyroid adenoma was surgically excised in 3/17 patients and F-18-FCH PET/MR was confirmed to be true positive by parathormone washout in 2/17 patients. In 12/17 positive cases, patients were clinically accepted as true positive and are now candidates for surgery. Histopathological results could not be obtained due to short follow up period.

Conclusion: F-18-FCH PET/MR is an effective method for preoperative localisation of parathyroid adenomas where neck USG and Tc-99m MIBI scintigraphy are negative. F-18 FCH PET/MR may also be considered as an effective tool in patients whom F-18FCH has also failed.

Keywords: PET/CT, hyperparathyroidism, radionuclide imaging

[BOP-34]**Definition of Risk Factors of Oncocytic Variant of Papillary Thyroid Carcinoma: Introspection into a Little-Known Subtype**

Kürşat Okuyucu¹, Engin Alagöz¹, Semra İnce¹, Serhan Mahmudov¹, Özdeş Emer¹, İbrahim Demirci², Aslı Ayan¹, Murat Urkan³, Bengül Günalp¹, Salih Devci⁴, Alper Özgür Karacalıoğlu¹, Nuri Arslan¹

¹University of Health Sciences, Gülhane Training and Research Hospital, Clinic of Nuclear Medicine, Ankara

²University of Health Sciences, Gülhane Training and Research Hospital, Clinic of Endocrinology, Ankara

³University of Health Sciences, Gülhane Training and Research Hospital, Clinic of General Surgery, Ankara

⁴University of Health Sciences, Gülhane Training and Research Hospital, Clinic of Pathology, Ankara

Aim: Oncocytic variant (OV) is an unusual subtype of papillary thyroid cancer whose histopathologic diagnostic criteria, clinicopathologic features and biological behavior are different and have not been

comprehensively studied, characterized in literature. Previous studies present conflicting results upon its prognosis. We investigated demographic and clinicopathologic risk factors effecting its prognosis while presenting our clinical experience.

Method: This is a retrospective cohort study reviewing 101 patients of OV from an archive of 4500 well-differentiated thyroid cancer treated with I-131 between 1991 and 2017. Predefined parameters of age, gender, tumor size (TS), total I-131 dose, time to recurrent disease, overall survival, extrathyroidal extension, multifocality, vascular invasion, accompanying other variants, capsular status of thyroid gland, initial cervical lymph node (LN) metastasis, preablation stimulated thyroglobulin level, background thyroiditis, stage were evaluated by statistical comparison between metastatic and nonmetastatic groups.

Results: Seventeen cases (17%) developed metastasis/recurrence, 70% of the recurrences occurred before 24 months. Four patients (4%) died during the follow-up. Metastatic sites were usually cervical LNs, local recurrence in thyroid bed and lungs. Multivariate analysis revealed stage (4) and TS were the main parameters impacting recurrence/metastasis. In the follow-up, isolated cervical LN metastasis was found in 41% of metastatic cases, while 12% had sole recurrence in thyroid bed. 88% of the metastatic disease included locoregional (cervical) and/or remote LNs. The recurrences were associated with initial thyroid masses greater than 3.5 cm in diameter.

Conclusion: We found that the prognosis of OV is not poor in our series. Stage (4) and TS are the main risk factors in metastatic development.

Keywords: Oncocytic variant, papillary thyroid cancer, predefined risk factors, recurrence, metastasis.

[BOP-35]**Diagnostic Contribution of Thyroid Scintigraphy to Dual Phase Parathyroid Scintigraphy in Detecting Parathyroid Adenoma**

Mustafa Genç¹, Elif Özdemir¹, Berna Evranos Ögmen², Zuhar Kandemir², Nilüfer Yıldırım², Şeyda Türkölmez²

¹Ankara Yıldırım Beyazıt University Faculty of Medicine, Department of Nuclear Medicine, Ankara

²Ankara Yıldırım Beyazıt University Faculty of Medicine, Department of Endocrinology and Metabolism, Ankara

³Ankara City Hospital, Clinic of Nuclear Medicine, Ankara

Aim: Parathyroid adenoma (PA) is the most common cause of primary hyperparathyroidism (PHP). Treatment of choice is minimally invasive surgery guided preferably by preoperative localization of the PA with imaging methods among which are parathyroid scintigraphy (PS) and ultrasonography (US). PS can be performed with different protocols such as dual phase Tc-99m-MIBI imaging, dual phase Tc-99m-MIBI imaging + Tc-99m pertechnetate imaging. In this study, the diagnostic contribution of Tc-99m pertechnetate thyroid scintigraphy to dual phase Tc-99m-MIBI PS and US was evaluated in patients who underwent surgery for PHP.

Method: Among 547 patients referred to our clinic with the diagnosis of PHP, 138 patients (F: 120, M: 18, mean age: 56) who were operated after scintigraphic imaging were retrospectively evaluated. Thyroid scintigraphy was performed with Tc-99m pertechnetate in a separate session in addition to early and late phase Tc-99m-MIBI imaging. Dual phase Tc-99m-MIBI images were evaluated by nuclear medicine physician who was experienced in PS interpretation. Thereafter, dual phase Tc-99m-MIBI PS images were reevaluated together with thyroid scintigraphy. Histopathology was accepted as the gold standard. Diagnostic parameters for dual-phase Tc-99m-MIBI imaging, dual-phase Tc-99m-MIBI imaging + thyroid scintigraphy and US were evaluated.

Results: Sensitivity, specificity, positive predictive value and diagnostic accuracy values for dual phase Tc-99m-MIBI imaging alone, dual-phase Tc-99m-MIBI imaging + thyroid scintigraphy and US are shown in the Table 1. Accordingly, when compared with US, PS alone was found to be inferior to diagnose PA. The addition of thyroid scintigraphy to standart-of-care PS significantly increased both the sensitivity and specificity of the latter in diagnosing PA and the combined imaging modality turned out to be superior to US. And the difference between dual phase Tc-99m-MIBI imaging and dual-phase Tc-99m-MIBI imaging + thyroid scintigraphy's diagnostic accuracies was statistically significant ($p<0.001$).

Conclusion: The combined use of thyroid scintigraphy and PS increases the diagnostic yield of PS alone for the detection of PA and thus may guide minimally invasive surgery in this patient population.

Keywords: Parathyroid scintigraphy, parathyroid adenoma, thyroid scintigraphy, Tc-99m-MIBI dual phase, diagnostic contribution, detecting

Table 1.

	Sensitivity	Specificity	Positive predictive value	Diagnostic accuracy
US	89.9%	37.9%	84.4%	78.9%
Tc-99m-MIBI	70.6%	68.9%	89.5%	70.2%
Tc-99m-MIBI + Tc-99m	83.4%	75.8%	92.8%	81.8%

US: Ultrasonography

[BOP-36]

The Value of Tc-99m-MIBI SPECT/CT Imaging in Post-op Follow-up of Differential Thyroid Cancer

Berna Okudan, Nazım Coşkun

University of Health Sciences, Ankara Numune Training and Research Hospital, Clinic of Nuclear Medicine, Ankara

Aim: The treatment of differentiated thyroid cancer (DTC) is surgery, iodine therapy and thyroid stimulating hormone (TSH) suppression. After total thyroidectomy, it should be evaluated for residual or metastasis. The aim of this study was to evaluate the use of Tc-99m-MIBI single photon emission computed tomography (SPECT)/CT imaging (scintigraphy) to determine the choice of DTC treatment and treatment response.

Method: Twenty one patients who underwent Tc-99m-MIBI scintigraphy and underwent total thyroidectomy with the diagnosis of DTC between 2017 and 18 were included in that study. Three patients were excluded from the study because their ultrasonography (USG) findings could not be reached. For scintigraphy; after the 15mCi Tc-99m-MIBI injection, images were taken at 10th and 150th minutes (SPECT/CT with head and neck static and planar scan). The findings were evaluated as residual and lymphadenopathy (LAP).

Results: Eighteen patients (15 females, 3 males; age: 45.3±12.6 years) were included in the study. The mean post-op Tg values of the patients were 70.21±279.32 ng/mL (0, 40-1189; reference interval: 0-60 ng/mL). In terms of residues, scintigraphic and USGic findings were compatible in 10 (55%) of them ($p=0.02$), and USG and scintigraphy results were not compatible in 8 patients (45%). In 3 (16%) of these patients, while residual thyroid

tissue was present on USG, no residual tissue was observed in scintigraphy. Two patients (11%) had residual thyroid tissue on scintigraphy and no residual tissue was detected on USG. Accordingly, 11 (55%) patients had residual tissue and LAP in SPECT/CT. In terms of LAP; in 7 patients, USG and scintigraphy were exactly the same (5 none/none), in 7 patients negative positive scintigraphy was negative, in 1 patient negative scintigraphy was positive and in 3 patients both positive but localization was different ($p=0.84$)

Conclusion: Tc-99m-MIBI SPECT/CT can be used in combination with USG in the decision of DTC post-op treatment. Tc-99m-MIBI is very advantageous in terms of patient comfort with its physical characteristics, its suitability for imaging and its easy preparation, low cost, less radiation exposure and not being affected by the serum TSH level (not cutting the levothyroxine and preventing hypothyroidism symptoms before imaging). Furthermore, in functional and non-functional metastases, the disadvantage of I-131 in non-functional or dedifferentiated Tc metastases is that it does not affect the I-131 treatment by not creating a "stunning" effect, may be an option.

Keywords: Thyroid cancer, MIBI, SPECT/CT

[OP-37]

Assessment of FDG PET/MR Findings in Terms of Hippocampal Volume and Metabolism in Temporal Lobe Epilepsy

Kerim Şeker¹, Ümit Özgür Akdemir¹, Seda Gülbahar¹, Uğuray Aydos¹, İrem Yıldırım², Gökhan Kurt², Neşe İlgin Karabacak¹, Lütüfye Özlem Atay¹

¹Gazi University Faculty of Medicine, Department of Nuclear Medicine, Ankara

²Gazi University Faculty of Medicine, Department of Neurology, Ankara

³Gazi University Faculty of Medicine, Department of Neurosurgery, Ankara

Aim: In temporal lobe epilepsy (TLE), brain F-18 fluorodeoxyglucose (FDG) positron emission tomography (PET) shows ipsilateral hippocampal hypometabolism. In parallel, magnetic resonance imaging (MRI) shows hippocampal volume loss and signal changes due to sclerosis. In this study, we aimed to evaluate the correlation between hippocampal metabolism and gray-matter volume and to determine the diagnostic accuracy of these parameters in the lateralization of TLE.

Method: The brain FDG PET/MRI findings of drug-resistant TLE patients who were scheduled for surgical treatment were evaluated retrospectively. Brain FDG PET and volumetric (3D) T1-weighted MRI data of 16 patients with a mean age of 34.4±7.8 (mean ± standard deviation) were recorded on a hybrid PET/MRI camera (Signa PET/MR, GE Healthcare). PET and MRI data were spatially normalized and MRI data were then segmented to measure gray matter volumes using the statistical parametric mapping software (SPM12, Wellcome Center for Human Neuroimaging). Asymmetry indices [$AI = (\text{left hemisphere} - \text{right hemisphere}) / (\text{left hemisphere} + \text{right hemisphere}) * 200$] of both hippocampi were calculated for both PET and MRI. Accordingly, the negative and positive AI values indicated left and right hippocampal lateralizations. Linear correlations of AI values for PET and MRI were determined. Finally, the results of lateralization based on the AI data were compared with the clinical lateralization.

Results: The ratio of clinically diagnosed left/right TLE was 8/8. According to the AI values calculated from FDG PET and MRI images, 14/16 (87.5%) and 13/16 (81.2%) of the patients could be correctly lateralized (Cohen's kappa were 0.750 and 0.625), respectively. PET and MRI findings were concordant in 13/16 (81.2%) of the patients. In addition, AI values obtained from these two methods were highly correlated (Pearson correlation coefficient=0.928; $p<0.001$).

Conclusion: Hippocampal hypometabolism observed in FDG PET and gray-matter loss observed in MRI are highly correlated with each other and both findings have high diagnostic accuracy in the lateralization of epileptogenic focus in TLE patients. PET and MRI findings can be evaluated objectively in terms of regional asymmetry with quantitative analysis. In order to compare the diagnostic accuracy of these two methods, larger patient series whose lateralization is finalized according to the follow-up findings are needed.

Keywords: Temporal lobe epilepsy, ippocampus, gray-matter volume, FDG, PET/MRI

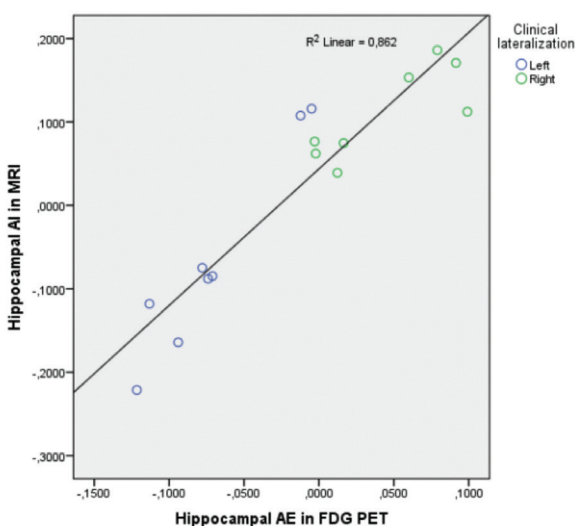


Figure 1. Linear correlation between the calculated asymmetry indices values for hippocampi in fluorodeoxyglucose positron emission tomography and gray-matter segmented magnetic resonance imaging
 FDG PET: Fluorodeoxyglucose positron emission tomography, MRI: Magnetic resonance imaging

[BOP-38]

Radiolabeled Antibody-coated Magnetic Nanoparticles: A Possible Therapeutic Approach

Aljosa Stankovic¹, Marija Mirkovic¹, Magdalena Lazarevic²

¹University Clinical Centre of the Republic of Srpska, Center for Biomedical Research, Banja Luka, Bosnia and Herzegovina

²Vinca Institute of Nuclear Sciences, Laboratory for Radioisotopes, Belgrade, Serbia

Aim: Magnetic nanoparticles (MNP) have great potential for medical applications due to their ability to enhance magnetic resonance imaging contrast and unique facile surface modification properties. MNPs functionalized with different antibody represent good carrier of diagnostic and therapeutic radionuclides. Surface modification of MNPs with radiopharmaceutical ligand such as 2,3-dimercaptosuccinic acid (DMSA) as well as aminosilans [e.g. 3-aminopropyltriethoxysilane (APTES)], facilitates their further functionalization (with different antibody, protein etc.) since they possess big amount of carboxylic and amino groups. The aim of this study was to design MNPs coated with DMSA and APTES, optimised the conditions for further conjugation with antibody labelled with therapeutic radionuclide (¹³¹I), assess their *in vitro* stability and explore their potential

application as radiopharmaceutical agent for dual therapy (hyperthermia and radionuclide therapy).

Method: Fe₃O₄ MNPs were synthesized using single step co precipitation method. The obtained MNPs functionalized with DMSA and APTES were characterized by X-ray diffraction, Fourier transform infrared spectroscopy and dynamic light scattering. The heating efficiency of MNPs was quantified through the specific power absorption (SPA) measurements. Radiolabeling of the antibody was carried out with different amount of ¹³¹I iodine using modified chloramine-T method. The radiolabeling yield of the antibody-MNP complex was determined using thin-layer chromatography. *In vitro* stability studies were tested in saline (0.9% NaCl) and human serum.

Results: The obtained SPA values of the aqueous dispersion of Fe₃O₄-DMSA and Fe₃O₄-APTES MNPs (23.9 kA/m, 397/577 kHz) were 124 W/g and 205 W/g, respectively. Results indicate possible use of coated MNPs in hyperthermia treatment. Both types of coated MNPs were conjugated with ¹³¹I-antibody in a reproducible high yield (≥98%) and exhibited high *in vitro* stability (≥97%) in saline and human serum after 48 hours.

Conclusion: Surface bioengineering of nanomaterials based on Fe₃O₄ involving DMSA and APTES as coating ligands appears to be highly promising due to their colloidal stability in physiological media and big number of bonds with ¹³¹I radiolabeled antibodies. The SPA values and *in vitro* stability studies of radiolabeled MNPs exhibited favourable properties that justify further investigations toward their potential use as a dual therapy agent for hyperthermia and radionuclide therapy.

Keywords: Magnetic nanoparticles, radiolabeled antibody, hyperthermia, radionuclide therapy

8th BNMC ORAL PRESENTATIONS 4

[BOP-41]

New Sentinel Lenf Nodu Phantom for Outline Body Imaging Technique

Milena Dimcheva, Aleksandra Jovanovska

Cancer Center of Sofia, Russia

Aim: A disadvantage of lymphoscintigraphic studies is the absence of anatomic information in the images. While the backlighting imaging technique creates an outline of the patient's body. Several methods are in use for outlining the body contour during lymphoscintigraphy imaging with their own advantages and drawbacks. The aim of this study is to present the newly developed Sentinel lymph node (SLN) phantom allowing imaging at each acquisition time point images: anterior, lateral, and 45° anterior oblique in patients with SLN in breast carcinoma and patients with clinically localized melanoma.

Method: A dual-head gamma-camera system with large field-of-view (FOV) detectors was used to acquire planar emission and, if desired, single-photon computed tomographic (SPECT) or SPECT/CT images. Low energy, high-resolution (LEHR) collimators was used. The energy window is 15% centered on the 140 keV photopeak of Tc-99m. The acrylic phantom was used for body contouring to offer an accurate localization of the sentinel lymph nodes. The phantom was filled with homogenous solution of 37 MBq Tc-99m albumin nanocolloid. The phantom was placed on the lower camera head of a dual-head camera, underneath the patient, and an anterior body outline image was acquired on the upper head. Lateral images are

also acquired with the patient lying supine, with her/his arm on the side with cancer (R/L) extended.

Results: The sentinel lymph nodes were detected in 82 cases and confirmed with the surgical gamma probe - Europrobe 3 during the surgical procedure.

Conclusion: Presurgical localizing of the sentinel nodes has become more accurate and is being performed with greater confidence with the new SLN phantom for outline body imaging technique. The overall sensitivity of the study for visualization remains the same with the other phantoms, but presentation is far superior and informative. The SLN phantom used for this purpose does not affect the acquisition data and does not lead to false negative results.

Keywords: Sentinel lymph node biopsy, melanoma, breast tumor, SLN phantom

[BOP-42]

Clinical Efficacy of Radiosynoviorthesis in Ankle and Wrist Joints with Systemic Arthritis

Ioannis Plakovou, Zimmy Kotrotsios, Euanthia Giannoula, Christos Sachpekidis

Academic Dpt Of Nucler Medicine, Papageorgiou Hsp

Aim: To retrospectively evaluate the long-term efficacy of radiosynoviorthesis (RSV) in patients with systemic arthritis (rheumatoid or psoriatic arthritis) of the ankle and wrist joints.

Method: Thirty-one painful despite pharmacotherapy ankle (19) and wrist (12) joints of 30 patients (28 females, 69.8±4 years) enrolled the study. They were intra-articularly injected with 2mci of 169Er citrate. In the pretherapeutic bone scan, all joints presented an positive blood pool image, indicative for active local synovitis. Joint functional status and pain were assessed by a visual analog scale (VAS of ten steps: 1-lack of any impairment to 10-total disability) just before (less than 12 days) and at least a month after treatment, with a mean follow-up of 24 months.

Results: Twenty-seven in 27 patients (90%) reported a pronounced improvement in their manual activities. The mean total score of 8.1+/-1.5 prior to treatment decreased significantly to 2.9+/-1.8 after RS (p<0.05). Ankle joints were more frequently reported to be resistant to therapy than wrist joints.

Conclusion: RSV is highly effective in ankle and wrist joint systemic arthritis active synovitis.

Keywords: Radiosynoviorthesis, systemic synovitis, arthritis, RSO, RSV

[BOP-43]

Clinical Feasibility of Late Lu-177 PSMA Scanning After Lu-177 PSMA I&T Therapy

Türkay Hekimsoy, Gözde Dağlıöz Görür, Serkan İşgören, Hakan Demir

Kocaeli University Faculty of Medicine, Department of Nuclear Medicine, Kocaeli

Aim: Lu-177 prostate-specific membrane antigen (PSMA) is a promising agent used both for treatment of metastatic castration-resistant prostate cancer (mCRPC) and post-treatment scanning. Even though it is advised to perform a whole body scan one day after therapy, sometimes it is not possible to do it due to several reasons. The purpose of our study is to investigate the feasibility of late scanning 3 days after Lu-177 PSMA I&T therapy.

Method: Sixteen patients with mCRPC (mean age 71.8±8 years old) who underwent Lu-177 PSMA I&T therapy between March 2018 and December 2018 were included in this study. A total of seventy-two Lu-177 PSMA whole body scans which were performed one day and three days after Lu-177 PSMA I&T therapy were investigated retrospectively. Mean administered activity per cycle was 5.4±0.4 GBq. Whole body planar images were performed one day and three days after each therapy. Regions of interest (ROI) were obtained of right parotid gland, liver, proximal thigh and metastatic lesion which has the highest Lu-177 PSMA I&T uptake from first and third day images. Maximum counts of each ROI were noted. ROI of the proximal thigh was accepted as background. Retention indexes (maximum count of early image normalized ROI/maximum count of late image normalized ROI) of ROIs between early and late images were evaluated. Additionally, patients were divided into two groups according to serum total prostate-specific antigen (PSA) level decline or increase after each cycle. Retention indexes of all ROIs were compared with 2 groups.

Results: When normalized to background, there was significant difference between liver and right parotid gland ROI counts of early and late images but there was no significant difference between metastatic lesion counts (p=0.86). Retention indexes of liver, right parotid gland and metastatic lesion were significantly different (p<0.001). When comparing serum total PSA change after each therapy with retention indexes of metastatic lesions, no significant correlation was detected (p=0.76).

Conclusion: Our analysis indicates that performing Lu-177 PSMA I&T whole body scan on patients 3 days after therapy is clinically feasible when it is not possible to perform one day after therapy. According to our results, retention index of the metastatic lesion may not be used as a prognostic tool for Lu-177 PSMA therapy response but larger studies are required.

Keywords: Lu-177 PSMA therapy, metastatic castration-resistant prostate cancer, Lu-177 PSMA scan

[BOP-44]

Effect of External Cooling on Lu-177 Prostate-specific Membrane Antigen Uptake for Parotid Glands

Burcak Yılmaz¹, Serap Nişli¹, Nurhan Ergül¹, Rıza Umar Gürsu², Ozgur Açıkgoz², Tefvik Fikret Cermik¹

¹University of Health Sciences, İstanbul Research and Training Hospital Department of, Nuclear Medicine, İstanbul

²University of Health Sciences, İstanbul Research and Training Hospital Department of, Medical Oncology, İstanbul

³University of Health Sciences, Kanuni Sultan Suleyman Research and Training Hospital, Department of Medical Oncology, İstanbul

Aim: Metastatic castration-resistant prostate cancer (mCRPC) patients have been started to treat with prostate-specific membrane antigen (PSMA) targeted radioligand therapy (PRLT), especially with Lu-177 PSMA-617 in recent years. But, side effects of PRLT against salivary glands, limits the treatment safety. Current study aims to show the effect of external cooling with icepacks on Lu-177 PSMA-617 uptake in parotid glands (PGs).

Method: Nineteen patients (Mean age 72.9 years) who had pre-treatment Ga-68 PSMA-11 pozitron emisyon tomografi (PET)/CT with mCRPC referred for the first time for Lu-177 PSMA-617 treatment were included in this prospective study from May 2018 to October 2018. Maximum and mean standard uptake values (SUV_{max} and SUV_{mean}) of right (R) and left (L) PGs were measured on Ga-68 PSMA PET/CT before treatment and without icepack applications. Before the initiation of PRLT, frozen icepacks were fixated unilaterally (all right sided) on PGs of patients and applied approximately 5 hours. Fourth and 24th h of PRLT, whole body planar scintigraphy and

4th hour head/neck region SPECT/CT were acquired after injection of Lu-177 PSMA-617. Region of interest (ROI) for R and L PGs were calculated. Furthermore volume of interest (VOI) of SPECT counts and volume of CT of 4th hour R and L PGs were calculated.

Results: Before the PRLT, Ga-68 PSMA-11 PET/CT scan without icepack application, showed no statistical significance between R and L PGs' SUV_{max} or SUV_{mean} variables ($p>0.05$). In the 4th and 24th hour of PRLT, on the planar images externally cooled R PGs' ROI's did not demonstrated any statistical difference when compared with L PGs which were not externally cooled ($p>0.05$). SPECT/CT images in the 4th hour of PRLT, had no statistical difference between R and L PGs' VOI counts. In addition, volumes of R and L PGs had not shown any statistical difference between the glands ($p>0.05$).

Conclusion: It has been shown that the application of ice packs for external cooling during the Lu-177 PSMA-617 injection does not have any effect on the radioligand uptake of PGs. Prospective studies and alternative methods, in order to prevent PRLT effects on salivary glands and xerostomia are mandatory.

Keywords: Lu-177, PSMA, prostate cancer, parotid, ice-pack

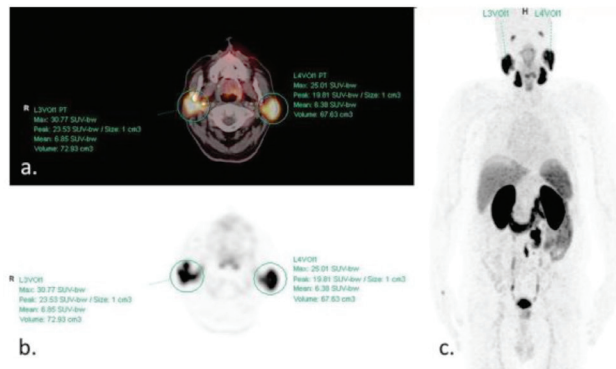


Figure 1. Ga-68 PSMA PET-CT

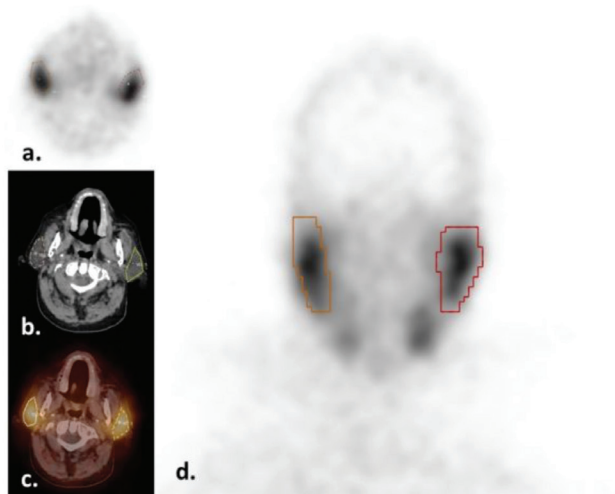


Figure 2. Lu-177 PSMA SPECT-CT

Table 1: Statistical analysis according to ice-pack application

Variable	p value	95 % CI	Std. Deviation
R/L PG Planar (4 th hour)	0.572	-1619 - 2841	4626.75
R/L PG Planar (24 th hour)	0.314	-495 - 1456	2023.65
R/L PG SPECT (4 th hour)	0.270	-10582 - 3144	14239.43
R/L PG CT Volume (4 th hour)	0.481	-1261 - 2573	3977.60
R/L PG SUV _{mean}	0.524	-0.67 - 1.27	2.00
R/L PG SUV _{max}	0.575	-2.13 -1.22	3.47
R-C/L-C PG Planar (4 th hour)	0.104	-.074 - .722	0.8
R-C/L-C PG SUV _{mean}	0.556	-2.5 - 4.56	7.4
R-C/L-C PG SUV _{max}	0.08	-2.39 - .13	2.6

R: Right, L: Left, PG: Parotid gland, SPECT: Single Photon emission computed tomography, CT: Computed tomography, SUV: Standard uptake value, Std: Standart, CI: Confidence interval

[BOP-45]

The diagnostic value of hybrid SPECT/CT lung scintigraphy in pulmonary embolism

Nilüfer Yıldırım¹, Mustafa Genç¹, Elif Özdemir², Şeyda Türkölmez², Ayşegül Gözalan³

¹Ankara Atatürk Training and Research Hospital, Clinic of Nuclear Medicine, Ankara

²Yıldırım Beyazıt University, Ankara

³İstanbul Ümraniye Training and Research Hospital, Clinic of Microbiology, İstanbul

Aim: Pulmonary perfusion scintigraphy is mainly used to exclude pulmonary embolism (PE). SPECT has largely replaced planar imaging for evaluation of PE, however hybrid scanner with computerized tomography (CT) allows both perfusion and ventilation data in the same session. In this study; we evaluated the diagnostic value of SPECT/CT scintigraphy in the diagnosis of PE and to compare this method with planar and SPECT methods.

Method: Data of 108 consecutive patients, suspected of having PE and underwent perfusion scintigraphy, were retrospectively collected. All patients have planar and SPECT images for perfusion data, chest radiograph and low-dose CT (LDCT) for ventilation data. Interpretation was performed according to the criteria suggested in European Association of Nuclear Medicine (EANM) guidelines by 2 nuclear medicine physicians as PE, No PE and nondiagnostic for PE. Final diagnosis of disease was based on the clinical decision and/or evaluation of a 12 months follow-up period.

Results: The diagnostic performance parameters of SPECT/LDCT were as follows; sensitivity 96.8%, spesificity 90.7%, positive predictive value 93.8% and negative predictive value 95.1%. There were only 2 (1.9%) patients with nondiagnostic findings for PE with SPECT/LDCT and 9 (8.3%) patients with SPECT perfusion and chest radiograph, however there was 33 (30.6%) with planar perfusion and chest radiograph. Using tomographic images, it was possible to determine 73% of nondiagnostic findings with planar images. This ratio raised to 94% with SPECT/LDCT. The agreement between three methods were moderate to strong with highest kappa value was 0.84 for SPECT and SPECT/LDCT.

Conclusion: Lung perfusion scintigraphy performed with a hybrid SPECT/LDCT method has an excellent diagnostic efficacy for PE, as well as the least nondiagnostic findings as compared with planar and SPECT scintigraphy.

Therefore, the precision of pulmonary embolism in a single session makes this method advantageous for PE, due to the urgency of the disease.

Keywords: SPECT/CT, lung perfusion, pulmonary embolism

[BOP-46]

Evaluation of Concurrency of Mechanical Contractions in Cases with Left Ventricular Diastolic Dysfunction

A. Özgür Karacaloğlu, Alev Çınar, Engin Alagöz, Nuri Arslan

University of Health Sciences, Gülhane Training and Research Hospital Clinic of, Nuclear Medicine, İstanbul

Aim: In gMPS applied cases, simultaneity of left ventricles' mechanical contractions is evaluated by phase analysis. In this study, it was aimed to investigate whether the concomitant left ventricular mechanical contraction was impaired in patients with diastolic dysfunction.

Method: Images of patients who applied to our clinic for gMPS with a pre-diagnosis of CAD between August 2018/February 2019 were retrospectively reviewed. Stress gMPS imaging is performed, on patients who reached maximum effort during cardiac stress test or imaging of solid-state cardiac gamma camera (GE 630, Haife Israel) after 30 ± 10 min after injection of 296-370 MBq (8-10 mCi) Tc-99m MIBI during injection of pharmacological agent according to the two-day protocol. Images were analyzed using ECtoolbox (Emory Uni. Atlanta, USA) software. Eleven patients with diastolic dysfunction according to Peak Filling Rate (PFR) and time to peak filling rate (TTPFR) as cardiac dysfunction parameters (DD+) (PFR<2 and TTPFR \geq 180 ms) and 10 patients without diastolic dysfunction (DD-) (PFR \geq 2 and TTPFR <180 ms). (11 women, age range: 42-78) in total of 21 patients were included in the study. And in this case, five quantitative parameters were obtained by using phase analysis with the software above and the difference between the groups was investigated.

Results: In the DD + group, respectively, Peak Phase (PP): 164.09 ± 20.613 , Standard Deviation (SD): 36.47 ± 13.37 , Bandwidth (BW): 110.09 ± 48.93 , Histogram Skewness (HS): 2.73 ± 0.70 , Kurtosis Histogram (HK): 9.17 ± 5.54 have been found. In the DD-group, respectively, PP: 150.6 ± 23.37 , SD: 19.43 ± 6.62 , BW: 55.1 ± 15.82 , HS: 3.76 ± 1.11 , HK: 18.09 ± 13.11 have been found. Groups were compared with each other in terms of PP, SD, HB, HS and HK values and the difference between the values of SD ($p < 0.05$); HB ($p < 0.01$); HK ($p < 0.01$) was statistically significant. No significant difference was found between PP and HS values.

Conclusion: In patients with diastolic dysfunction, concurrency of left ventricular mechanical contraction was found to be impaired. The preliminary findings of an ongoing study appear to open new doors to the assessment of left ventricular function with gMPS.

Keywords: Gated myocard perfusion scintigraphy, phase analysis, diastolic dysfunction

[BOP-47]

A Novel Patient-Based Dosimetric Approach for Y-90 Microsphere Treatment

Feryal Çakır¹, Murat Fani Bozkurt², Ayşe Kevser Özden²

¹Hacettepe University Institute of Science, Ankara

²Hacettepe University Faculty of Medicine, Ankara

Aim: Yttrium-90 (Y-90) microsphere treatment is an internal radiation treatment in which hepatic tumors are selectively targeted via arterial route owing to unique circulation pattern of the liver. One major questionable aspect of this treatment is the heterogeneity of intra-tumoral microcirculation and its effect on therapy response as well as the amount of activity to provide maximum tumor dose along with minimum background dose. This study aims to give a vision to uncover these issues with use of a novel patient-based dosimetric approach.

Method: A total of 90 treatments which were performed with Y-90 glass microspheres in the same university hospital between the years 2012 and 2018 were re-planned retrospectively based on a novel personalised, patient-based dosimetric approach. During planning, a software that provides a voxel-based dosimetric approach through anatomical and functional sequence images of the patient was used. The retrospective dosimetric re-planning for each patient gave an evaluation in terms of targeted effective tumor dose and critical organ doses. The relation between Y-90 glass microsphere activities and perfused tissue volume, perfused tumor volume and absorbed doses was investigated. The planning steps of the software used in this study were reviewed in terms of parameters that would affect the dosimetric results, and a standard was specified for these parameters followed by comparison with those that were calculated pre-therapy with semi-dosimetric approach.

Results: Novel patient-based retrospective plannings showed that the amount of Y-90 glass microsphere activity, which were used under current conditions and calculated taking a reference of absorbing a dose of 120 Gy of the lobar volume alone, were lower than the pre-calculated activity for 14 /90 (~16%) therapies and higher for 76 /90 (~84%) therapies when considering the critical organ tolerance doses.

Conclusion: This study showed that the patient-based dosimetric approach, taking into account the anatomic variation of the relevant patient, different tumor size and its localization, is of vital importance with respect to provide maximum tumor dose along with minimum background dose in accordance with the logic of internal radiation treatment. The findings of this preliminary study will be expected to give rise to proceed with clinical studies in order to optimize treatment efficiency.

Keywords: Radioembolization, hepatic artery, patient-based dosimetry, absorbed dose

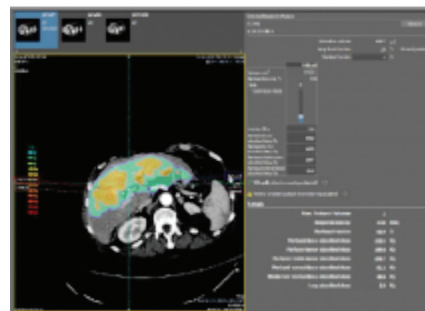


Figure 1. Multi-compartment dosimetry modul of the software

[BOP-48]

Is There Relationship Between ST2 Level and Myocardial Perfusion Scintigraphy in the Evaluation of Myocardial Ischemia?

Seyit Ahmet Ertürk¹, Zekiye Hasbek¹, Tuba Çandar²

¹Sivas Cumhuriyet University Faculty of Medicine, Department of Nuclear Medicine, Sivas

²Ufuk University Faculty of Medicine, Department of Medical Biochemistry, İstanbul

Aim: Early markers of cardiovascular disease are important in order to minimize the negative consequences of this disease and to guide emergency interventional procedures. Troponin and BNP (brain natriuretic peptide), one of the most frequently used biomarkers in the routine, may be elevated in many different clinical conditions. Recently, there has been studies that a protein called ST2 (suppression of tumorigenicity 2) is an important prognostic biomarker that can be used in ischemic heart disease in particular. ST2 is a biomarker that is secreted secondary to cardiomyocyte tension and it is in interleukin-1 receptor family, which is soluble and has transmembrane isoforms. This protein is expressed in stressed viable myocardial tissue. However, the function of ST2 in CAD is still unclear. The aim of this study was to evaluate the relationship between the presence/absence of ischemia in myocardial perfusion scintigraphy (MPS) and serum ST2 levels. Our second aim was to evaluate the relationship between ST2 levels and automated analysis parameters like left ventricular ejection fraction (LVEF), summed stress score (SSS), stress myocardial perfusion defect percentage (stress extent) and transient ischemic dilatation (TID) which are obtained from MPS.

Method: There were 104 patients in this prospective study (65F, 39M, mean age: 59.5) who underwent myocardial perfusion scintigraphy with Tc-99m-MIBI with a doubt of myocardial ischemia. Patients with COPD, malignancy, renal failure, cardiac surgery other than CAD were not included in our study. ~ 2 cc blood was taken during intravenous catheter application for MPS and plasma was separated by centrifugation. ST2 levels was measured quantitatively in ASPECT Reader using ASPECT-PLUS ST2 test.

Results: There was no statistically significant difference between the mean ST2 levels of ischemic patients (21.53±13) and patients without ischemia (22.32±12) (p=0.755). ST2 levels of 28 male patients with ischemia were higher than female patients, but were not statistically significant (p=0.253) (Table 1). No statistically significant relationship was found between ST2 level and quantitative automated analysis parameters of MPS in terms of stress extent, SSS, TID and stress EF (p=0.970; 0.677; 0.429; 0.850, respectively).

Conclusion: There was no significant relationship between ST2 level and MPS findings in the evaluation of myocardial ischemia. However larger prospective studies are needed.

Keywords: ST2, myocardial ischemia, scintigraphy

Table 1. Presence of ischemia in MPS and its relationship with ST2 levels

		n (%)	ST2 Levels	p
Ischemia	Present	46 (44.2)	21.53±13	0.755
	Absent	58 (55.8)	22.32±12	
Patients with ischemia	Female	18 (39.1)	18.72±12	0.253
	Male	28 (60.9)	23.34±13	

8th BNMC ORAL PRESENTATIONS 5

[BOP-51]

The Interaction of Pre-Treatment F-18 FDG PET/CT Metabolic Parameters in Colorectal Cancer and Microsatellite Instability

Burcak Yılmaz

University of Health Sciences, İstanbul Research and Training Hospital, Clinic of Nuclear Medicine, İstanbul

Aim: Microsatellite instability (MSI) and defective mismatch repair (MMR) system were described as beneficial tumor features for response to immune therapy. The aim of this study is to determine the interaction between MSI and pre-treatment metabolic F-18 fluoro-deoxy-glucose (FDG) positron emission tomography/computed tomography (PET/CT) parameters among patients with operated colorectal cancer (CRCa) and to predict overall survival (OS).

Method: A total of 2007 F-18 FDG PET/CT images of histopathologically verified patients with CRCa at a single institution for 5 years were identified from our PET console electronic database. Patients with previous or concurrent diagnosis of any other primary malignancy were excluded from the study. One hundred eighty two patients who had staging PET/CT examination were further evaluated and of those, 50 patients (14 female, 36 male; mean age 62.0±10.1, range 40-82 years) who underwent pre-operation F-18 FDG PET/CT with histopathologically analyzed MSI status were included in the current study. F-18 FDG PET/CT metabolic parameters [metabolic tumor volume (MTV), tumor lesion glycolysis (TLG), maximum standard uptake value (SUV_{max})] for the primary tumor area and/or mesenteric/para-aortic lymph nodes and also accompanying distant metastases were reported. The expression of the MMR proteins MLH1, MSH2, MSH6, and PMS2 were analyzed using immunohistochemistry. The overall survival, pre-treatment metabolic PET parameters and other histopathological parameters for patients with detected MSI and without MSI were compared.

Results: The median follow-up period was 25.5±14 months (range=1-60 months). Overall, 8/50 patients showed MSI with at least 2 microsatellite markers gave positive results for each patient. Eight exitus were observed and only 1 patient with MSI died in the 4th month of follow up. five-year OS was 83.3% vs 87.5% in patients without MSI vs with MSI. ROC curve analyses could not demonstrate a cut off value with high sensitivity and specificity to verify MSI for PET parameters. MSI status was not a prognostic factor in univariate analysis for OS either. Additionally, independent t-test showed significance only for T-MTV and distance metastasis existence for MSI status (p=0.04).

Conclusion: T-MTV and distance metastasis existence may be a predictive factor for predicting MSI status among F-18 FDG PET/CT parameters but further prospective studies is mandatory.

Keywords: Colorectal cancer, F-18 FDG-PET/CT, metabolic parameters, microsatellite instability, overall survival

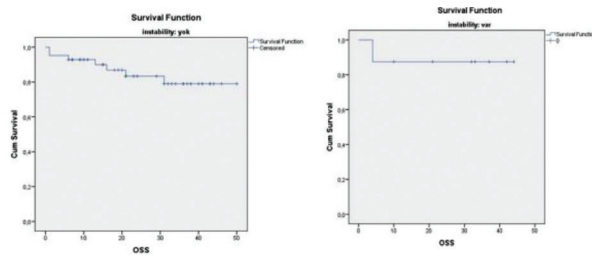


Figure 1. Overall survival of colorectal cancer patients with and without microsatellite instability

[BOP-52]

Metabolic Parameters of Staging FDG PET/CT Correlates with Poor Prognosis in Patients with Nasopharyngeal Cancer

Burcu Esen Akkas, Büşra Bedriye Demirel, Özge Öz, Emre Hüseyin Tosun, Gülin Uçmak

University of Health Sciences, Ankara Oncology Research and Training Hospital, Clinic of Nuclear Medicine, Ankara

Aim: The aim of this study was to test the predictive power of staging FDG PET/CT for future recurrence and disease progression in patients with nasopharyngeal carcinoma (NC) treated with definitive therapy.

Method: Eight patients with NC, who underwent nasopharyngeal MRI and PET/CT imaging for staging were included. All patients had squamous cell carcinoma. Staging were performed according to TNM. Metabolic parameters of PET such as maximum standardized uptake value (SUV_{max}), SUV_{peak} , metabolic tumor volume (MTV) and total lesion glycolysis (TLG) were recorded. Definitive radiotherapy and/or chemotherapy were administered according to NCCN guideline. After treatment, all patients underwent standard follow-up procedure with physical examination, diagnostic work-up including MRI and PET/CT at 3-6th month post-treatment. At the final visit, based on patient outcome, patients were grouped as disease free (D0) and patients with residual/progressive disease (D1). Metabolic parameters of staging PET/CT were correlated with Tstage, Nstage and with patient outcome.

Results: We observed significant positive correlation between Tstage and tumor SUV_{max} , SUV_{peak} , MTV and TLG ($p=0.001$). Nstage were correlated only with tumor TLG ($p=0.03$). SUV_{max} and SUV_{peak} of involved nodes were correlated with Nstage. We observed higher nodal FDG uptake in higher Nstages, $p=0.02$. Mean follow-up period was 33 months (12-80 months). Forty patients were free of disease, 6 patients had local disease, 13 patients had progressive disease and metastasis. Both Tstage and Nstage were inversely associated with clinical remission ($p=0.004$). Tumor SUVs and nodal SUVs were not correlated with the final clinical status. However, higher MTV ($p=0.02$) and TLG ($p=0.008$) were significantly correlated with progressive disease on follow-up. Among all metabolic parameters, TLG had the strongest correlation with poor prognosis with the narrowest confidence interval. ROC curves demonstrated that if 135 is chosen as the cutoff value, the sensitivity and specificity of PET/CT in predicting progressive disease was 85% and 71%, respectively with the area under the curve: 0.88.

Conclusion: Higher MTV and TLG at the initial presentation predict worse prognosis and shorter disease free survival in patients with NC. Further prospective studies are warranted in order to evaluate the need for more aggressive treatment strategies for NC patients with higher MTV and TLG scores.

Keywords: Nasopharyngeal cancer, prognosis, PET/CT, total lesion glycolysis, metabolic tumor volume, SUV_{max}

[BOP-53]

A Comparison of Adopted and Modified Cut-off Values of SUV_{max} to Characterize Solitary Pulmonary Nodule on F-18 FDG PET/CT

Serkan Güngör

Istanbul Medeniyet University Faculty of Medicine, Department of Nuclear Medicine, Istanbul

Aim: Characterization of solitary pulmonary nodule (SPN) is necessary to choose an appropriate treatment approach on time. There is variation in cut-off value of SUV_{max} used among different institutions for discriminating benign from malignant SPNs. The first F-18 florodeoksiglukoz (FDG) pozitron emisyon tomografi (PET/CT) publications frequently adopted 2.5 as a cut-off value for SUV_{max} . The aim of this study is to evaluate the diagnostic accuracy of adopted and modified cut-off values of SUV_{max} to identify the one with the highest diagnostic value in guiding the differential diagnosis of SPNs.

Method: A retrospective review of F-18 FDG PET/CT scans from 83 patients with SPN confirmed by pathology or clinical follow-up were included. The diagnostic values of PET/CT metabolic (SUV_{max}) and volumetric (size, CT volume, Hounsfield Units, and 3D ratio) parameters were calculated to detect malignancy. In addition, the classical criteria of 2.5 SUV_{max} cut-off was compared with the modified SUV_{max} cut-off value in terms of diagnostic accuracy. PET/CT parameters were assessed using the Receiving Operating Characteristic analysis.

Results: There were 38 benign and 45 malignant SPNs (median age: 61 ± 13 years, mean nodule size: 19.3 ± 6 mm). The metabolic and volumetric parameters showed significantly higher values in the malignant lesions compared with the benign lesions except for the 3D ratio which was higher in the benign lesions (Table 1). SUV_{max} demonstrated the highest area under the curve (AUC) of 0.97 among the all parameters. The ROC curve analysis showed the highest sensitivity for SUV_{max} at modified cut-off value of 3.6 and adopted cut-off value of 2.5. However, the specificity, PPV, NPV, and the accuracy were found higher at cut-off value of 3.6 than the adopted cut-off value of 2.5. The ROC curve analysis of all PET/CT parameters in characterizing SPN is shown in the Table 2 and the Figure 1.

Conclusion: We found that the optimal cut-off value of SUV_{max} to predict malignancy in SPNs was 3.6. Although the classical criteria of 2.5 SUV_{max} cutoff is very sensitive for malignant nodules, it has a high falsepositive rate and reduced specificity when characterizing SPNs. Our results can support the hypothesis that application of the higher cut-off value of SUV_{max} improves the diagnostic performance of F-18 FDG PET/CT for the evaluation of SPNs particularly in an endemic population with acute or chronic infectious/inflammatory diseases.

Keywords: Solitary pulmonary nodule, F-18 FDG PET/CT, SUV_{max} cut-off value

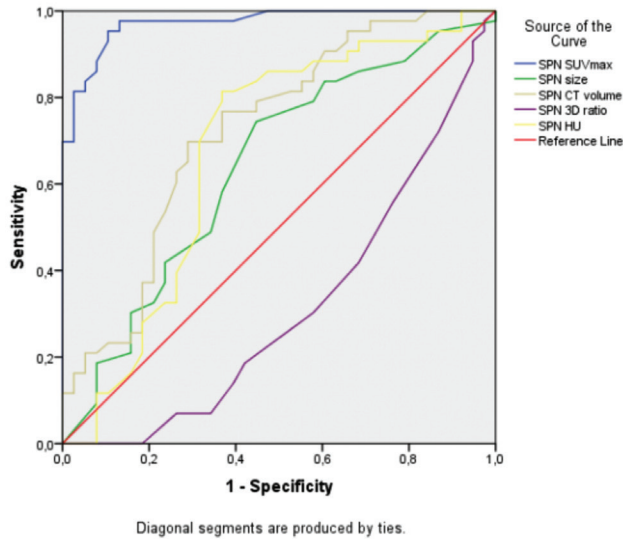


Figure 1.

Table 1. Comparison of PET/CT parameters between the benign and malignant lesion groups

	Benign group (n=38) X±SD orMed (IQR)*	Malignant group (n=45) X±SD orMed (IQR)*	p value**
SUV _{max}	2.3±1.4	8.7±3.8	<0.001
Size (mm)	17.9±6.0	20.6±5.8	0.049
CT volume(cm ³)	2.8±2.4	4.8±3.7	0.004
3D ratio	1.5±0.4	1.2±0.3	0.002
HU	-20 (-73.0-9.2)	3.0 (-8.0-12.0)	0.007

PET/CT: Positron emission tomography, IQR: Interquartile range

Table 2. ROC curve analysis of PET/CT parameters in characterizing solitary pulmonary nodules (n=83)

	Sensitivity (%)	Specificity (%)	PPV (%)	NPV (%)	Accuracy (%)	AUC (%)	Cut-off value
SUV _{max} for cut-off 3.6	97.7	86.8	89.6	94.3	91.6	0.97	3.6
SUV _{max} for cut-off 2.5	97.7	63.2	75.4	92.3	80.7	0.97	2.5
Size (mm)	74.4	55.3	65.3	65.6	65.4	0.64	17.5
CT volume (cm ³)	76.7	63.2	70.2	70.6	70.4	0.72	2.75
3D ratio	72.1	13.2	48.4	29.4	44.4	0.31	1.05
HU	81.4	63.2	71.4	75.0	72.8	0.67	-11.5

ROC: Receiver operating characteristic, PET/CT: Positron emission tomography,

[BOP-54]

Beyond SUVmax. MTV and TLG on Histopathological Subtypes of Esophageal Cancer

Ulku KORKMAZ¹, Muhammet Bekir Hacıoglu², Gülay Durmus-Altun¹

¹Trakya University Medical Faculty, Department Of Nuclear Medicine

²Trakya University Medical Faculty, Department Of Medical Oncology

Aim: F-18 fluorodeoxyglucose (F-18 FDG) positron emission tomography (PET) combined with computed tomography (CT) scans are standard in the staging of Esophageal cancer (EC) for detect metastatic disease. Histopathological subtypes of tumors are known to alter prognosis and metabolic behavior. In this study, we investigated the answer to two questions. First of them whether a difference between the histopathological subtypes of EC (adenocarcinoma and SCC) in terms of standardized uptake value (SUV_{max}), metabolic tumor volume (MTV) and total lesion glycolysis (TLG) obtained by PET/CT, and the second whether a correlation between prognosis and any of these parameters?

Method: We retrospectively reviewed records of patients diagnosed and followed with EC between 2009 and 2016 at Medical Oncology Department. We assessed their PET/CT images for calculate the metabolic parameters and investigated relationship of these with histopathological subtypes of EC.

Results: Fifty three patients were included in the study. Primary tumours were predominantly located in the distal esophagus (%77.4). There was no significant association with lesion SUV_{max}, neither overall survival (OS) nor progression free survival (PFS). The MTV of the primary tumor was associated the histopathological subtype and MTV values of esophageal adenocarcinoma (EAC) significantly higher than esophageal squamous cell cancer (ESCC) (cut of value >27.7; Sensitivity= 52.4% and Specificity= 90.5%). MTV (30.7±20.5 for adenocancer, 21.8±22.6 for SCC, p= 0.017), TLG (285.7±264 for adenocancer, 213.3±378.7 for SCC, p=0.068).

Conclusion: This study, showed the MTV values related to histopathologic subtype. On the other hand, there was no significant difference between adenocarcinoma and squamous cell carcinoma subtypes, clinical staging and TLG and SUV_{max} values.

Keywords : : Adenocancer; Difference; Esophageal cancer; PET/CT; Squamous cell cancer; SUVmax; MTV; TLG

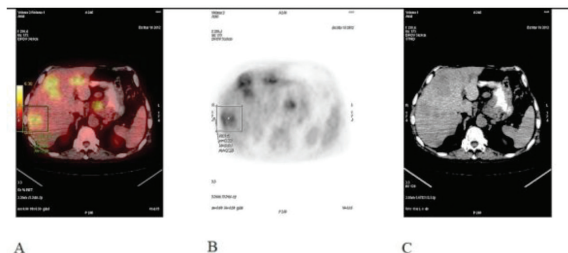


Figure 1.

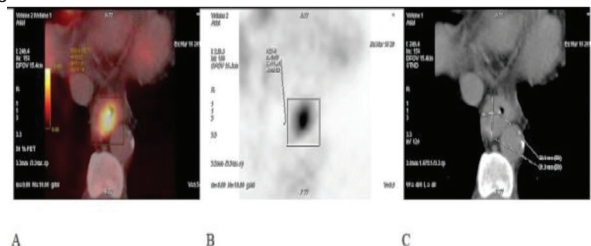


Figure 2.

Table 1. Cut-off values for MTV and TLG

	Cut-off	AUC	p	Sensitivity (%)	Specificity (%)
Primary MTV	>27.7	0.715	0.009	52.4	90.5
Total MTV	>26.9	0.710	0.011	76.2	66.7
Primary TLG	>133.4	0.646	0.059	72.0	64.3

MTV: Metabolic tumor volume , TLG: Total lesion glycolysis

Table 2.

mean±SD	All (n=53)	EAC (n=25)	ESCC (n=28)	P value
SUVmax g/dL	13.96	12.7 ± 4.4	15.1 ± 7.6	0.390
MTV	26.25	30.7 ± 20.5	21.8 ± 22.6	0.017
TLG	247.44	285.7 ± 264	213.3 ± 378.7	0.068

[BOP-55]

Intraoperative Sentinel Node Evaluation with Scintigraphy Assisted Frozen After Neoadjuvant Treatment in Breast Cancer

Kezban Berberoglu¹, Ayhan Erdemir², Kemal Rasa², Huseyin Baloglu³, Metin Cakmakci²

¹Anadolu Medical Center, Clinic of Nuclear Medicine, Istanbul

²Anadolu Medical Center, Clinic of General Surgery, Istanbul

³Anadolu Medical Center, Clinic of Pathology, Istanbul

Objective: Intraoperative identification of axillary metastasis is important since it may effect the decision for the type of operation, either to add axillary resection or not. This study aimed to evaluate the value of scintigraphy assisted intraoperative sentinel lymph node evaluation with frozen section after neoadjuvant chemotherapy.

Method: A total of 80 patients who underwent neoadjuvant chemotherapy for breast cancer with axillary metastasis were included in this study. Axillary metastasis had been shown by pozitron emisyon tomografi (PET/CT) and ultrasound guided fine needle aspiration biopsy. Two hours prior to surgery, patients underwent Tc-99m nano-colloid axillary sentinel lymph node scintigraphy and 1-4 sentinel lymph nodes were labeled. Intraoperatively, the surgeon identified the sentinel nodes using a gamma probe and resected for frozen section. Patients with positive frozen section pathological examination results underwent axillary dissection, whereas a limited lymph node sample was obtained in patients with negative frozen result for further pathological examination. All samples underwent routine pathological examination to show the presence of axillary metastasis.

Results: Frozen section was positive in 32 (40.0%) of the cases. On the other hand, 41 (51.3%) cases had axillary metastasis on postoperative pathological examination. Sensitivity, specificity, positive predictive value, and negative predictive value of scintigraphy assisted intraoperative evaluation for predicting pathologically confirmed axillary metastasis were 80.5%, 100%, 100%, and 82.3%, respectively. Based on this strategy, 48.8% of patients avoided unnecessary axillary dissection since frozen section yielded true negative result, when compared to a strategy using dissection in all cases.

Conclusion: Scintigraphy assisted intraoperative axillary evaluation seems to be a promising strategy, particularly in terms of preventing unnecessary axillary dissection. However, sensitivity of this method needs to be improved to reduce the number of false negative cases.

Keywords: Breast cancer, neo-adjuvant chemotherapy, sentinel lymph node scintigraphy, intra-operative frozen

[BOP-56]

Lymphoscintigraphic Evaluation of Lymphatic Insufficiency After Total Knee Arthroplasty

Hümevra Gencer¹, Kürsat Gencer², Seyhan Karaçavuş¹, Firat Ozan²

¹University of Health Sciences, Kayseri City Hospital, Clinic of Nuclear Medicine, Kayseri

²Health Sciences University Kayseri City Hospital, Clinic of Orthopedics and Traumatology, Kayseri

Aim: Extremity swelling is one of frequent complications of total knee arthroplasty (TKA). There are many causes of this condition but in long term follow up, ongoing or progressive swelling may point out lymphatic insufficiency. Lymphatic flow and sites of lymph drainage can readily be evaluated with lymphoscintigraphy. Lymphoscintigraphy images easily demonstrate the unpredictability of lymphatic drainage patterns.

Method: Thirty seven patients (25/12 F/M; mean age 58.3) who underwent TKA (37 unilateral, 5 bilateral TKA) in Kayseri Education and Research Hospital between 2010-2016 and had unilateral extremity swelling in long term follow up were included in this study. Other causes of extremity swelling (venous insufficiency, infectious diseases etc.) were excluded. Lymphoscintigraphic imaging performed both lower extremities, pelvis and abdomen of patients. Dynamic scanning started just after injection of 1 mCi Tc-99m-labeled nanocolloid to first interdigital space of both feet followed by whole body imaging at 10th minutes, 1st and 4th hours. The scans were analyzed and scored for visualization and dilatation of main lymphatic vessels, regional and deep lymph nodes, collateral vessels and dermal back flow. Lymphoscintigraphic scoring was carried out for all patients as described in Table 1.

Results: We evaluate 42 extremities of 37 patients and show visualization of main lymphatic vessels in 38 (90.5%), collateral vessels in 26 (61.9%), deep lymphatic drainage (popliteal lymph nodes) in 18 (42.8%), dilatation of main lymphatic vessels in 12 (28.6%), dermal back flow in 16 (38%) and soon sufficient radiotracer uptake at regional lymph nodes in 35 (83%) extremities. According to the lymphoscintigraphic scoring system mean scintigraphic score was 6 (range 0-10). We demonstrate lymphatic drainage disorders or insufficiency in patients who were complained from discomfort and unexplained swelling after TKA. Based on these results appropriate treatment modality had planned.

Conclusion: Unreasonable pain, swelling and discomfort are displeased outcomes of TKA and finding underlying causes is critical for clinical guidance. Lymphatic mapping with lymphoscintigraphy can play a pivotal role in defining the etiology of extremity swelling and in predicting the success of common therapies.

Keywords: Total knee arthroplasty, lymphoscintigraphy, lymphatic insufficiency

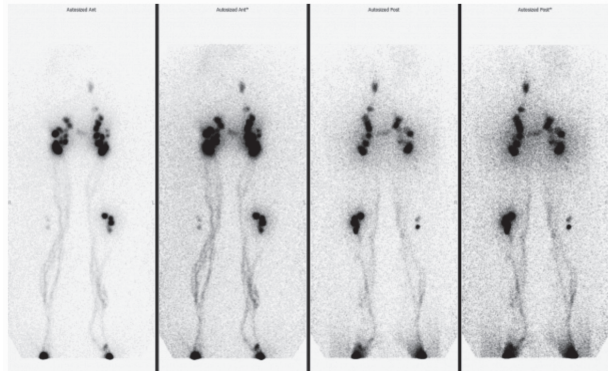


Figure 1. First hour whole body images of bilateral total knee arthroplasty patient

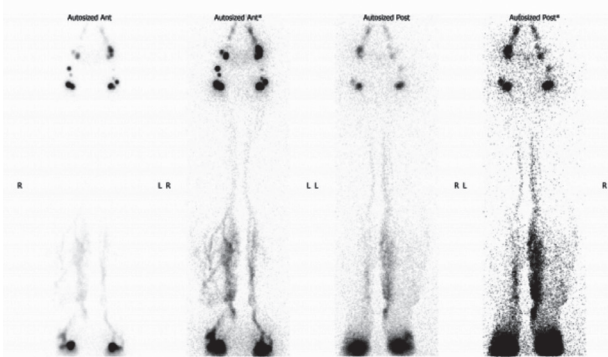


Figure 2. First hour whole body images of right total knee arthroplasty patient

Table 1. Scoring System

- A) Regional nodal uptake: 0: sufficient uptake at inguinal, iliak and paraaortic lymph nodes, 1: regional nodal uptake after postegzersize images 2: reduced nodal uptake at late images, 3: the lack of lymphatic transport to regional lymph nodes
- B) Dermal back flow: 0: no dermal back flow 1: small localized dermal back flow, 2: circumferantial dermal back flow including one segment of extremity, 3: circumferantial dermal back flow including more than one segment of extremity
- C) Visualization of main lymphatic vessels: 0: normal radiotracer passage to main lymphatic vessels, 1: no radiotracer transition to main lymphatic vessels
- D) Dilatation of main lymphatic vessels: 0: no dilated main lymphatic vessels, 1: dilated main lymphatic vessels
- E) Collateral circulation 0: no kollateral vessels, 1: visualized collateral vessels
- F) Deep lymphatic Drainage 0: no deep lymphatic system nodes, 1: visualized deep lymphatic system nodes

[BOP-57]

The Role of FDG-PET/CT in Re-Staging for Testicular Germ Cell Tumors Correlation with hCG, AFP, and LDH

Göksele Alçın¹, Esra Arslan¹, Tamer Aksoy¹, Rıza Umar Gürsu², Tevfik Fikret Çermik¹

¹Istanbul Research and Training Hospital, Clinic of Nuclear Medicine, İstanbul
²Istanbul Research and Training Hospital, Clinic of Medical Oncology, İstanbul

Aim: The aim of this study is to investigate the role of F-18 florodeoksiglukoz (FDG)- pozitron emisyon tomografi (PET/CT) in the restaging of germ cell testicular cancer with elevated tumor markers and treatment response assessment after chemotherapy.

Method: FDG-PET/CT study was performed in 36 patients (mean age±SD: 35.8±7.3 years) with germ cell testicular tumor in this retrospective study. FDG uptake was interpreted visually correlated with CT and when pathological FDG uptake or lymph node detected, the standardized uptake value was measured. Twenty two patient's histopathology were non-seminomatous germ cell tumors (NSGCTs) and 14 patient had seminomatous germ cell tumor (SGCT). An FDG-PET/CT scan was taken for restaging in seven SGCT patients and 9 NSGCTs patients with elevated tumor marker levels (hCG, AFP, and LDH). 7 SGCT patients and 13 NSGCTs patients underwent FDG-PET/CT imaging for treatment response assessment.

Results: In all patients who underwent FDG-PET/CT for restaging paraaortic metastatic lymph nodes were detected with high FDG uptake and SUV_{max} values were 5.1-34.1 (21.2±7.8). In NSGCTs group; SUV_{max} values of paraaortic lymph nodes were 5.1-34.1 (20.1±8.9) and 12.9-32.0 (22.7±1.4) in NSGCTs and SGCT group, respectively. The lymph node SUVmax values were higher in the patients as the tumor marker (hCG, AFP, and LDH) level increased and it was found to be statistically significant (p<0.05). Also, there was a significant correlation between the maximum diameter of the hypermetabolic lymph node and SUV_{max} values, tumor marker levels (p<0.05 and p=0.312, respectively). In the treatment response assessment patient group; neither SGCT nor NSGCTs patients had lymph nodes showing pathological FDG uptake. hCG, AFP, and LDH levels were significantly reduced compared to before treatment and were in normal levels.

Conclusion: FDG-PET/CT is an efficient hybrid imaging modality in restaging both SGCT and NSGCTs especially in markedly high tumor marker levels also in treatment response assessment.

Keywords : FDG-PET/CT, germ cell testicular cancer, tumor marker, SUV_{max}

[BOP-58]

The Results of Definitive External Radtotherapy and Brachytherapy in Patients With Medical Inoperabl Endometrium Cancer

Ebru Atasever Akkaş¹, Bektaş Kaya¹, Burcu Esen Akkaş³, Gülin Uçmak Vural²

¹University of Health Sciences, Dr. Abdurrahman Yurtaslan Oncology Training and Research Hospital, Department of Radiation Oncology, Ankara
²University of Health Sciences, Dr. Abdurrahman Yurtaslan Oncology Training and Research Hospital, Department of Nuclear Medicine, Ankara

Aim: We aimed to report the treatment and follow-up results of medical inoperable endometrial cancer patients who were treated for definitive purposes in our clinic.

Method: Between January 2010 and April 2017, the records of 894 patients with endometrial cancer treated in our clinic were evaluated

retrospectively. Of these, 14 patients with stage I-III endometrial carcinoma who were defined as medically in-operable and treated with three-dimensional (3D) high-dose (HDR) cuff brachytherapy (BRT) and / or external radiotherapy (ERT) for definitive purposes were included in this study. The results of the treatment were evaluated based on clinical follow-up results.

Results: The mean age was 65 years (51-84 years) and the median follow-up period was 32 months (7-13 months). Surgery could not be performed due to morbid obesity and cardiopulmonary disease in 6 patients (43%), due to multiple comorbid diseases such as coronary artery disease, chronic obstructive pulmonary disorder and diabetes in 7 patients (50%) and due to advanced patient age (n=1). Demographic characteristics of the patient and the tumor are given in Table 1. The Charlson comorbidity index (CCI) was median 6 (range 3-9). The median values for maximum standardized uptake value, median metabolic tumor volume and total lesion glycolysis were 27.3, 14.9 mL and 243 g for the patient group. The mean dose of BRT was given in $6,77 \pm 0.5$ Gy median 4 (3-5) fraction, ERT mean dose was 49.2 ± 2.5 Gy median 28 (25-28) fraction. In the third month after treatment, treatment response was found to be complete response 6 (42.9%), partial response 4 (28.6%), stable 1 (7.1%), progression 3 (21.4%). In three cases, pelvic recurrence developed after 22 months of treatment. Five cases died on follow up after the completion of the treatment, but the CCI indexes of these cases were also very high. The 1, 2, 5, and 8-year overall survival rates were 70%, 60%, 60%, 60% and the 2-year local control rate was 76%, respectively.

Conclusion: Surgery is the mainstay of treatment of endometrial cancer, the literature lacks of large series of patients treated only with definitive radiotherapy. In this relatively small patient series, we observed that ERT and 3D BRT may be used as well-tolerated treatment options for disease control and toxicity in non-surgical endometrial cancer patients who has metabolically active tumors detected on FDG PET/CT.

Keywords: Medical inoperable, endometrial cancer, radiotherapy, FDG PET/CT

Table 1. Patient and tumor characteristics

	n (% or range)
Total patients	14
Mean follow up (months)	32 (7-103)
Median age (range) (years)	66 (51-84)
Stage (%) I, II, III	9 (64.3), 2 (14.3), 3 (21.4)
Grade (%) 1, 2, 3	8 (57.1), 3 (21.4), 3 (21.4)
RT (%) EBRT, ICRT, EBRT+ICRT	3 (21.4), 1 (7.1), 10 (71.4)
ICRT applicator (%) Double tendem, Tendem+ovoid	7 (63.6), 4 (36.4)
ICRT technic (%) 2D, 3D	4 (28.6), 7 (50)
Pretreatment MRI (%) Available, Absent	8 (57.1), 6 (42.9)
Pretreatment PET (%) Available, Absent	5 (35.7), 9 (64.3)
Median weight (kg)	129 (75-136)
Median Pretreatment Hb (g/dL)	10.9 (10.1-14.1)
Median posttreatment Hb (g/dL)	11.5 (8.6-14.7)
Median Pretreatment Ca 125 (U/mL)	19.9 (15-24.96)
Median posttreatment Ca 125 (U/mL)	20.8 (16.5-25.21)
Median SUV _{max}	27.3 (28.8-30.8)
Median Metabolic Tumor Volume MTV (mL)	14.9 (10-19.9)
Median Total Lesion Glycolysis TLG (g)	243 (189.1-296.9)

MRI: Magnetic resonance imaging, MTV: Metabolic tumor volume